

The oncogenic function of PLAGL2 is mediated via specific target genes through a Wnt-independent mechanism in colorectal cancer

Anthony D. Fischer², Daniel A. Veronese Paniagua³, Shriya Swaminathan³, Hajime Kashima¹,
Deborah C. Rubin¹, Blair B. Madison^{1*}

¹Department of Medicine, Division of Gastroenterology, Washington University School of
Medicine, Saint Louis, MO 63110.

²Department of Genetics, Washington University School of Medicine, Saint Louis, MO 63110.

³Washington University School of Medicine, Saint Louis, MO 63110.

* Corresponding Author:

Email: bbmadison@gmail.com (BM)

ABSTRACT

Colorectal cancer (CRC) tumorigenesis and progression are linked to common oncogenic mutations, especially in the tumor suppressor *APC*, whose loss triggers the deregulation of TCF4/ β -Catenin activity. CRC tumorigenesis is also driven by multiple epimutational modifiers, such as transcriptional regulators. We describe the common (and near-universal) activation of the zinc finger transcription factor and Let-7 target PLAGL2 in CRC and find that it is a key driver of intestinal epithelial transformation. PLAGL2 drives proliferation, cell cycle progression, and anchorage-independent growth in CRC cell lines and non-transformed intestinal cells. Investigating effects of PLAGL2 on downstream pathways revealed very modest effects on canonical Wnt signaling. Alternatively, we find pronounced effects on the direct PLAGL2 target genes *IGF2*, a fetal growth factor, and *ASCL2*, an intestinal stem cell-specific bHLH transcription factor. Inactivation of PLAGL2 in CRC cell lines has pronounced effects on *ASCL2* reporter activity. Furthermore, *ASCL2* expression can partially rescue deficits of proliferation and cell cycle progression caused by depletion of PLAGL2 in CRC cell lines. Thus, the oncogenic effects of PLAGL2 appear to be mediated via core stem cell and onco-fetal pathways, with minimal effects on downstream Wnt signaling.

INTRODUCTION

Colorectal cancer (CRC) is the third most common of all human malignancies and is the second leading cause of cancer-related deaths, after lung/bronchus cancer (seer.cancer.gov/statfacts). For over 20 years, the role of canonical Wnt signaling has been front and center for this malignancy, given the key role of the gatekeeper tumor suppressor, *APC*, which encodes a key scaffold protein in the β -Catenin destruction complex [1, 2]. Mutations in other Wnt pathway components, such as *AXIN2*, *CTNNB1*, and *RSPO* genes [3]

can also lead to hyperactive Wnt signaling in CRC. Mutations in *TP53*, *SMAD4*, and *KRAS* are also very common in CRC, underscoring the roles of pathways regulating genome integrity, TGF β /SMAD, and MAPK signaling. However, additional pathways are relevant in CRC pathogenesis, especially those pathways that drive an immature, fetal, or stem cell expression signature; such signatures predict an aggressive phenotype and poor prognosis [4, 5].

The Let-7 family of microRNAs (miRNAs) are well known for their key role in repressing naïve cellular states, controlling proliferation, and for maintaining cellular differentiation [6-9]. Consistent with this role Let-7 depletion promotes stem cell fate in intestinal epithelial cells [10] while down-regulation of Let-7 miRNA levels (or compromised Let-7 activity) fuels CRC carcinogenesis [10-12], with similar pro-oncogenic effects in many other malignancies [13-17]. Targets repressed by the Let-7 miRNA family are often part of proto-typical onco-fetal pathways that are frequently re-activated in a multitude of malignancies [8], including CRC [18, 19]. Such targets include *IGF2BP1*, *IGF2BP2*, *HMGA2*, *MYCN*, and a target we have recently characterized, *PLAGL2* [20]. We have previously documented the integral role of the Let-7 target HMGA2 in driving tumorigenesis in mouse models of intestine-specific Let-7 depletion [10], although HMGA2 alone does not appear to drive stem cell fate in intestinal epithelial cells [10]. In contrast, we discovered that *PLAGL2* clearly drives stem cell fate in intestinal organoids, and directly activates the key stem cell-specific transcription factor, *ASCL2* [20]. *ASCL2* is critical for establishing and maintaining intestinal stem cell fate [21, 22].

Previous studies have demonstrated some oncogenic roles for *PLAGL2* in CRC cell lines, with some documented effects on features of cellular transformation, *in vitro* [23-27]. Although these effects are hypothesized to be mediated via *PLAGL2* enhancement of canonical Wnt signaling [23-27], the effects on Wnt signaling are often modest and the specific roles for such effects have not been determined. Studies in human CRC and glioma cells have revealed that *PLAGL2* directly activates expression of *WNT6* [27, 28]. Despite this, effects on downstream Wnt signaling were not documented following manipulation of either *PLAGL2* or

WNT6 in CRC cell lines [27], whereas a clear effect was seen in neural stem cells [28]. This may reflect the commonplace ligand-independent hyperactivation of canonical Wnt signaling that occurs in CRC, e.g. from mutations in *APC*, which likely obscures (or renders irrelevant) any effects of individual upstream Wnt ligands. Further insight into the relationship between PLAGL2 and Wnt signaling was gained from experiments where we manipulated PLAGL2 levels in intestinal organoids [20]. PLAGL2 over-expression conferred Wnt-independent growth, but did not consistently augment Wnt signaling [20]. These results contrast the PLAGL2 studies described above, which hypothesize an obligatory downstream role for Wnt signaling in the context of cellular transformation. In non-transformed cells (organoids) we did find that factors (perhaps Wnt ligands) secreted from PLAGL2-overexpressing organoids enhanced a Wnt reporter in co-cultured organoids [20]. Consistent with this, PLAGL2 over-expression robustly activated expression of several Wnt ligands in organoids [20].

To investigate oncogenic mechanisms downstream of PLAGL2 we examined the potential of PLAGL2 to drive and maintain features of cellular transformation, and how such effects were mediated by direct PLAGL2 target genes. We find that PLAGL2 is a commonly up-regulated factor in CRC and has significant transforming properties. PLAGL2 effects on ASCL2-mediated signaling appear much more robust than effects on Wnt signaling. Through a close examination of TCF4/ β -Catenin target genes and a TOP-tdT Wnt reporter, we find that PLAGL2 has minimal effects on canonical Wnt signaling. Consistent with these findings, over-expression of the PLAGL2 target genes *ASCL2* and *IGF2* (but not constitutive activation of Wnt signaling) can rescue proliferation defects caused by PLAGL2 inactivation.

RESULTS

We first examined expression of *PLAGL2* in matched colonic adenocarcinomas to compare expression between tumors and non-malignant tissue from the same individual.

PLAGL2 expression was usually undetectable in non-tumor tissue (Fig 1A), whereas in tumor tissue *PLAGL2* was universally up-regulated (Fig 1A). Consistent with this, analysis of TCGA RNA-seq data for colorectal cancer revealed the common and robust up-regulation of *PLAGL2* in tumor tissue (Fig 1B). Expression analysis in CRC cell lines revealed *PLAGL2* expression in all CRC cell lines tested, with robust expression in HEK293T cells (Fig 1C). Further examination of TCGA data revealed that *PLAGL2* over-expression is a frequent feature of chromosomal instability (CIN) microsatellite-stable (MSS) tumors ($P = 3.7\text{e-}17$), a class that makes up the majority (~80%) of CRCs. This is consistent with data from TCGA [29-31], where we find that the only mutations significantly associated with *PLAGL2* over-expression are *TP53* ($P < 0.0001$) and *APC* ($P < 0.01$) (Fig 1D), which are hallmarks of CIN tumors [29]. This close association with *APC* loss could underlie observations that *PLAGL2* expression correlates with β -Catenin levels in tumors [25]. As expected, *PLAGL2* up-regulation is rarely seen in tumors with mutations in *BRAF*, *ACVR2A*, *TGFBR2*, *MSH6*, or *MSH3* ($P < 0.0001$), which are typical in MSI tumors [29].

Fig 1. *PLAGL2* is turned on in the majority of colorectal cancers and is predictive of overall survival. A) *PLAGL2* mRNA expression in 10 pairs of colon adenocarcinomas, with matched non-tumor adjacent tissue, as previously described [10]. **B)** *PLAGL2* expression in non-tumor and colorectal adenocarcinoma tumors from the TCGA PanCancer Atlas cohort [69] **C)** RT-PCR assay quantifying relative levels of *PLAGL2* mRNA in colorectal cancer cell lines and HEK293T cells. **D)** Oncoprint showing mutation and expression profiles of commonly mutated cancer genes, including *PLAGL2*, from the TCGA PanCancer Atlas of colorectal adenocarcinomas. **E)** Overall survival of CRC patients stratified for high expression of *PLAGL2* (>3 SD above mean) relative compared to all other tumors, based on microarray expression data [29]. **F)** Overall survival of CRC patients stratified for high expression of *PLAGL2* (>2 SD above mean) compared to low expression (>2 SD below mean) based on microarray expression data

(TCGA Provisional). Statistical significance was evaluated using Student's paired t-test **(A)**, Student's one-tailed t-test **(B)**, or a Mantel-Cox log-rank test **(E, F)**.

To determine effects on disease outcomes, tumors were stratified for expression of PLAGL2 using data from two CRC TCGA cohorts, and analyzed for overall survival. In both cohorts, high expression of PLAGL2 in tumors predicted significantly reduced survival of CRC patients (Fig 1E, F). Thus, PLAGL2 is commonly turned on in CRC tumors, with high-level expression likely driving more aggressive disease progression.

We previously generated PLAGL2-mutant DLD1 cell lines [20] using SRIRACCHA [32] and here we examined their proliferation via a co-expressed H2BGFP reporter, which easily enabled their enumeration. Each mutant clone exhibited significant deficits in proliferation compared to non-mutant DLD1 parent cells (Fig 2A). While defined mutant clones generated with site-specific nucleases (such as CRISPR) can produce robust loss-of-function models, we also examined *PLAGL2* loss using CRISPR/Cas9 mutagenesis in a polyclonal population of mutant Caco2 and HT29 cells. Targeted cells were monitored using a transposon expressing a nuclear GFP reporter along with guide RNAs (gRNAs) against *PLAGL2* (Fig 2B). This transposon was delivered to cells already stably expressing EspCas9. In both Caco2 (Fig 2C) and HT29 (Fig 2D) cells, proliferation was significantly reduced in cells expressing the *PLAGL2*-specific gRNA. Lastly, shRNA knockdown of *PLAGL2* was pursued by a similar strategy with an shRNA-expressing transposon, along with a nuclear GFP reporter (Fig 2E). DLD1 cell lines established with this transposon revealed several shRNAs that robustly depleted *PLAGL2* mRNA (Fig 2F). In Caco2 cells expressing shRNA #3 and #4 (Fig 2G), proliferation was significantly reduced, especially for shRNA #4 (Fig 2H). Effects of *PLAGL2* knockdown were evaluated in the context of the FUCCI cell cycle reporter [33], delivered to cells using a transposon vector. In both Caco2 (Fig 2I) and HT29 (Fig 2J) cells, the FUCCI reporter revealed that *PLAGL2* knockdown decreased the number of cells in the S/G₂/M phases of the cell cycle,

but increased the number of cells in G₀/G₁. In sum, PLAGL2 depletion in CRC cell lines compromises proliferation and cell cycle progression.

Fig 2. Knock-down or knock-out of *PLAGL2* compromises proliferation and cell cycle progression in CRC cell lines. **A)** Proliferation of stable CRISPR-mutated *PLAGL2* mutant DLD1 clones [20] compared to parental DLD1 cells. **B)** PB vector for stable expression of gRNAs and NLS-GFP, with Puro resistance. Caco2 **(C)** or HT29 **(D)** cell lines stably expressing EspCas9 were transfected with a PB vector expressing nuclear GFP and a non-specific (NS) gRNA or a gRNA against *PLAGL2*, and then growth was monitored. **E)** PB vector for stable expression of shRNAs and NLS-GFP, with Puro resistance. **F)** Knock-down (KD) of *PLAGL2* was assessed by RT-PCR in DLD1 cells **(F)** and also confirmed in Caco2 **(G)**. **H)** Proliferation of Caco2 cells stably transfected with PB vectors expressing nuclear GFP and non-specific (NS) or *PLAGL2*-specific shRNAs. Cell cycle status using the FUCCI [33] reporter co-transfected with a non-fluorescent shRNA PB vector was evaluated in Caco2 **(I)** and HT29 **(J)** CRC cells. For **A-D**, and **H** proliferation was quantified through enumeration of fluorescently labeled nuclei expressing NLS-GFP. Statistical significance (*p<0.05 or **p<0.01) was evaluated through an ordinary one-way ANOVA and Dunnett's multiple comparisons post-hoc test.

Migration, invasion, and the ability to survive anchorage-independent growth are salient hallmarks of transformed cells. In transwell assays we evaluated migration in the DLD1 mutant clones and found that migration is severely compromised in both mutants (Fig 3A, D). Invasion through a layer of Matrigel was also remarkably reduced in DLD1 mutants, especially mutant #1 (Fig 3B, E, F). Knock-down of *PLAGL2* in Caco2 cells also reduced migration in transwell assays, especially for shRNA #4 (Fig 3C). Lastly, *PLAGL2* was over-expressed in IEC6 cells to evaluate anchorage independent growth in soft agar. *PLAGL2* O/E consistently enabled the growth and formation of colonies (Fig 3G, H), demonstrating that *PLAGL2* can confer resistance to anoikis-mediated cell death, a key property of transformed cells.

Fig 3. PLAGL2 drives migration, invasion, and colony formation in soft agar. Assays measuring migration **(A)** or invasion through Matrigel **(B)** of stable CRISPR-mutated *PLAGL2* mutant DLD1 clones [20] compared to parental DLD1. **(C)** Migration assay of Caco2 cells stably transfected with PB vectors expressing nuclear GFP and a non-specific (NS) or a *PLAGL2*-specific shRNA. Images of GFP-expressing cells that have migrated through porous trans-well membranes 24 hours after plating for parental DLD1 cells **(D)**, DLD1 mutant clone #1 **(E)** or mutant clone #2 **(F)**. Soft agar colony forming assay for IEC6 cells transfected with a PB empty vector **(G)** or a PB vector expressing *PLAGL2* **(H)**. Statistical significance (* $p < 0.05$ or ** $p < 0.01$) was evaluated through an ordinary one-way ANOVA and Dunnett's multiple comparisons post-hoc test.

We next investigated the role of specific *PLAGL2* target genes. *IGF2* encodes a critical fetal growth factor that has been demonstrated to be a direct *PLAG1* and *PLAGL2* target gene [34-36], but its role downstream of *PLAGL2* in the context of cellular transformation has not been investigated. Here we find that *IGF2* expression is significantly reduced in *PLAGL2* mutant DLD1 clones (Fig 4A) and following shRNA-mediated knockdown (Fig 4B). In SW480 cells we performed SRIRACCHA-enriched mutagenesis of *PLAGL2* with CRISPR/Cas9, delivered via transposon vector. RNA was extracted from a mixed polyclonal population of *PLAGL2* mutants for expression analysis, and mutagenesis of *PLAGL2* was confirmed by Illumina sequencing (S1 Fig). In this polyclonal population of *PLAGL2* mutants, *IGF2* expression was significantly reduced (Fig 4C). In defined clonal mutants, generated using CRISPR/Cas9 (also delivered via transposon vector) in mouse organoids [20] *Igf2* expression was also significantly reduced. Thus, *PLAGL2* is required for expression of *IGF2* in both transformed and non-transformed intestinal epithelial cells. Over-expression of *PLAGL2* in mouse organoids [20] resulted in robust dose-dependent up-regulation of *Igf2* mRNA (Fig 4E). In sum, *PLAGL2* appears necessary and sufficient to drive *IGF2* expression. To gauge effects of *IGF2* alone, the human *IGF2* cDNA was

over-expressed in mouse intestinal enteroids via transposon transgenesis (Fig 4F). IGF2 expression triggered organoid hyperplasia and the formation of large cysts (Fig 4G, H), which phenocopies the cyst-like appearance of PLAGL2-overexpressing enteroids [20].

Fig 4. PLAGL2 drives IGF2 expression in CRC cells and intestinal organoids and partially rescues growth phenotype in PLAGL2 mutant CRC cells. **A)** RT-PCR for *IGF2* in DLD1 PLAGL2 mutant clones. **B)** RT-PCR for *IGF2* in Caco2 cells following shRNA KD of PLAGL2. **C)** RT-PCR for *IGF2* following CRISPR/Cas mutagenesis using SRIRACCHA [32] and Hygromycin selection. **D)** RT-PCR for *Igf2* in *Plagl2* knockout mouse intestinal enteroids [20] compared to WT parental enteroids. **E)** RT-PCR for *Igf2* in 3 lines of mouse intestinal enteroids expressing low, medium, or high levels of human HA-tagged PLAGL2 [20] compared to empty vector control enteroids. **F)** RT-PCR for IGF2 mRNA following O/E in enteroids. **G+H)** Cyst-like morphology in IGF2 O/E enteroids. For comparison of more than 2 conditions the statistical significance (* $p < 0.05$ or ** $p < 0.01$) was evaluated through an ordinary one-way ANOVA and Dunnett's multiple comparisons post-hoc test. For pair-wise comparison, Welch's t-test was performed to determine statistical significance (* $p < 0.05$ or ** $p < 0.01$).

To investigate functional roles of PLAGL2 target genes, the downstream effectors *ASCL2* and *IGF2* were further examined in tumors and transformed CRC cell lines. We examined CRC tumors from the TCGA for expression correlation between PLAGL2 and ASCL2 target genes (*ASCL2*, *KLHDC4*, *OLFM4*, *RNF43*, *LGR5*, *MYB*, *NR2E3*, *SMOC2*, *OSBPL5*, and *SOX9*). Nine out of ten ASCL2 targets showed positive correlation with PLAGL2 in all three TCGA CRC cohorts, while most targets were also positively correlated with PLAGL2 in stomach adenocarcinoma and hepatocellular carcinoma tumors (Fig 5A). Consistent with this, CRC cell lines stratified for the lowest vs. highest quintile of PLAGL2 expression, as determined by previous RNA-seq studies [37], revealed that expression of ASCL2 is significantly higher in PLAGL2-high CRC cell lines (Fig 5B). SRIRACCHA-enriched mutagenesis of PLAGL2 in

SW480 cells (S1 Fig) also revealed depletion of *ASCL2* mRNA levels. This is all consistent with a role for *PLAGL2* in the direct transcriptional activation of *ASCL2*, as previously demonstrated in intestinal organoids and CRC cell lines [20]. However, to quantitatively gauge the impact on *ASCL2* activity in CRC cell lines we used the *ASCL2* reporter [38], adapted for transposon-mediated expression of tdTomato (STAR-tdT, Fig 5D). Co-transfection with shRNA vectors or an *ASCL2* vector revealed robust activation by *ASCL2* and modest reduction by shRNAs against *PLAGL2* (Fig 5E). After establishing stable transgenic lines, shRNA knockdown of *PLAGL2* caused a pronounced reduction in STAR-tdT reporter activity in SW480, HT29, and Caco2 cells (Fig 5F-H).

Figure 5. PLAGL2 activates an ASCL2-dependent program in CRC cells. A) Plots of correlation coefficients of linear regressions between *PLAGL2* and ten *ASCL2* direct target genes (*ASCL2*, *KLHDC4*, *OLFM4*, *RNF43*, *LGR5*, *MYB*, *NR2E3*, *SMOC2*, *OSBPL5*, and *SOX9*) for seven TCGA datasets, including 3 from CRC adenocarcinoma (AdCA), 2 from stomach AdCA, and 2 from liver hepatocellular carcinoma (HCC). **B)** Colorectal cancer cell lines (N=154 from [37]) were parsed into bottom and top quintiles for *PLAGL2* expression and then evaluated for *ASCL2* mRNA expression. **C)** EspCas9-mediated mutagenesis using SRIRACCHA [32] and gRNAs directed against LacZ or *PLAGL2*, followed by selection with hygromycin and RT-PCR for *ASCL2* mRNA. **D)** Depiction of the STAR *ASCL2* reporter construct. **E)** Activity of the stem cell *ASCL2* reporter (STAR-tdT) reporter [38] 48 hours after transfection in SW480 CRC cells that were also co-transfected along with vectors providing *PLAGL2* shRNA-mediated KD or *ASCL2* O/E. As expected *ASCL2* O/E augments STAR-tdT reporter activity. After selection with Puromycin for 6-8 days for stable *PLAGL2* shRNA expression STAR-tdT reporter activity (integral RFP fluorescence) was measured in SW480 **(F)**, HT29 **(G)**, and Caco2 **(H)** CRC cell lines. RFP levels were normalized to integral GFP fluorescence constitutively expressed by the PB shRNA vector. **I) FUCCI** analysis of cell cycling in Caco2 cells after shRNA mediated KD of *PLAGL2* and exogenous expression of *PLAGL2*, *ASCL2*, *IGF2*, *ASCL2* and *IGF2*, or a

constitutively active β -catenin. **J)** Rescue of DLD1 *PLAGL2* mutant clone #1 with IGF2 and/or ASCL2 O/E and assessment of colony size following selection with G418. **K)** Mutation profile of *PLAGL2* targeted with SRIRACCHA using eSpCas9 with simultaneous over-expression of ASCL2 or IGF2. For comparison of more than 2 conditions the statistical significance (* $p < 0.05$ or ** $p < 0.01$) was evaluated through an ordinary one-way ANOVA and Dunnett's multiple comparisons post-hoc test. For pair-wise comparison, Welch's t-test was performed to determine statistical significance (* $p < 0.05$ or ** $p < 0.01$).

If ASCL2 and/or IGF2 are critical drivers downstream of *PLAGL2*, then we expect that their expression would rescue growth following *PLAGL2* loss-of-function. We first examined proliferation using the FUCCI reporter following knock-down of *PLAGL2* and rescue with ASCL2 and/or IGF2. Only ASCL2 was able to restore cell cycle progression in Caco2 cells while neither IGF2 nor constitutively active β -Catenin (*CTNNB1*^{S33Y}) expression was sufficient (Fig 5I). Because of their expression of H2BGFP, DLD1 *PLAGL2* mutants could not be assessed using the FUCCI reporter. However, in *PLAGL2* DLD1 mutant line #1, ASCL2 and IGF2 individually augmented clone size following stable transfection, and when co-transfected together we observed synergistic effects between ASCL2 and IGF2 on growth in this *PLAGL2* mutant (Fig 5J), suggesting a role for both target genes. To examine a more diverse array of *PLAGL2* mutants, we performed SRIRACCHA-mediated mutagenesis [32] in Caco2 CRC cell lines while simultaneously providing PB-mediated transgenic expression of either IGF2 or ASCL2. If either IGF2 or ASCL2 is able to compensate for loss of *PLAGL2*, then we would expect increased survival and growth of clones with *PLAGL2* loss-of-function mutations if such clones also express exogenous IGF2 or ASCL2. Thus, a rescue would be evident in a higher proportion of *PLAGL2* mutants. Exogenous IGF2 expression does not result in a higher frequency of *PLAGL2* mutations, but surprisingly, ASCL2 expression results in a significantly lower frequency of *PLAGL2* mutations and higher proportion of non-coding mutations (Fig 5K). In a 2-step experiment where lines were first established that already over-expressed ASCL2 or IGF2,

PLAGL2 mutagenesis was not tolerated in Caco2 cells already over-expressing ASCL2; i.e. no clones were recovered, unlike IGF2 over-expressing or vector controls. This suggests that any oncogenic effects of ASCL2 depend on *PLAGL2*, and that these two factors may function as obligate partners.

Previous studies have reported that *PLAGL2* augments Wnt signaling [23, 24, 27], perhaps via the transcriptional activation of Wnt ligand genes [28]. To explore effects of *PLAGL2* on canonical Wnt signaling, we compared expression levels of *PLAGL2* mRNA with 36 Wnt target genes among 7 cancer datasets from the TCGA (Fig 6A). While some targets showed a positive correlation, many targets also showed anti-correlation with *PLAGL2*, and we observed no overall trend towards a positive association, except perhaps a slight positive correlation among liver hepatocellular carcinoma samples (Fig 6B). In addition, an examination of fold changes of these Wnt targets in RNA-seq data from *PLAGL2*-expressing intestinal organoids showed no clear trend (Fig 6C). In contrast, data sets directly manipulating Wnt signaling showed a clear decrease in Wnt target expression following β -Catenin knock-down or dnTCF4 expression, while stimulation of Wnt signaling in intestinal organoids (via GSK3 β inhibition) showed an induction of Wnt target gene expression (Fig 6C). Canonical Wnt signaling is also frequently measured via heterologous reporters. We used our TOP-tdT reporter [20] to quantify Wnt signaling in the context of *PLAGL2* knock-down. Co-transfection of dnTCF4 dramatically reduced signal from this reporter, as expected (Fig 6D). After establishing stable shRNA expression in the context of the TOP-tdT reporter, we observe a small decrease in normalized reporter signal in SW480 and Caco2 cells (Fig 6E, F), but not in HT29 cells (Fig 6G). Representative images from Caco2 experiments confirm modest effects on TOP-tdT signal (Fig 6H). Despite subtle effects in SW480 and Caco2 cells, no significant effects were observed on non-phosphorylated (“active”) β -Catenin or total β -Catenin protein levels in these cells (Fig 6I, J). In DLD1 *PLAGL2* mutant cell lines, similar effects were observed. Values were quantified from these immunoblot experiments (Fig 6 K-M). Expression analysis of Wnt target genes also

did not reveal any clear trend following *PLAGL2* knock-down (Fig 6N-P). SRIRACCHA-mediated mutagenesis of *PLAGL2* in SW480 cells (S1 Fig) and RT-PCR revealed a slight trend of reduced Wnt target gene expression, but only *ETS2* mRNA levels were significantly reduced (Fig 6Q, R). In sum, the data only support a small effect of *PLAGL2* on Wnt signaling in CRC cells.

Fig 6. Minimal effects on canonical Wnt signaling following inactivation of PLAGL2. A)

Heatmap of correlation coefficients for linear regressions between *PLAGL2* and 36 TCF4/ β -Catenin target genes for seven TCGA datasets, including 3 from CRC adenocarcinoma (AdCA), 2 from stomach AdCA, and 2 from liver hepatocellular carcinoma (HCC). **B)** Dot/scatter plots of data from **(A)**. **C)** Violin plots of fold changes among 28 TCF4/ β -Catenin target genes for conditions as follows: 1) between *PLAGL2*-low vs. *PLAGL2*-high CRC AdCA tumors (TCGA), 2) between control and KD of *CTNNB1* (β -Catenin) or inducible O/E of a dnTCF4 in LS174T CRC cell lines [70], and 3) GSK3 β inhibition and Wnt/TCF4/ β -Catenin activation in intestinal organoids following treatment with 5 μ M CHIR99021 [71]. **D)** Activity of the Wnt Super 8x TopFlash reporter [72] driving expression of tdT (TOP-tdT) 48 hours after transfection in SW480 CRC cells that were also co-transfected along with vectors providing *PLAGL2* shRNA-mediated KD or dnTCF4 O/E. As expected, dnTCF4 O/E reduces signal from the TOP-tdT reporter and reduces the number of RFP-positive cells. After selection with Puromycin for 6-8 days for stable *PLAGL2* shRNA expression TOP-tdT reporter activity (integral RFP fluorescence) was measured in SW480 **(E)**, Caco2 **(F)**, and HT29 **(G)** CRC cell lines. RFP levels were normalized to integral GFP fluorescence constitutively expressed by the PB shRNA vector. **H)** Representative images of fluorescent Caco2 cells after 6 days of selection with 10 μ g/mL puromycin. Active (non-phosphorylated) and total β -Catenin levels were measured following *PLAGL2* KD in SW480 **(I)**, Caco2 **(J)**, and *PLAGL2* mutant DLD1 clones **(K)**. Protein levels were quantified and normalized to tubulin **(L-N)**. Direct TCF4/ β -Catenin target gene expression levels

were measured by RT-PCR in SW480 and Caco2 cells following PLAGL2 KD (**O, P**), in *PLAGL2* mutant DLD1 clones (**Q**), and following SRIRACCHA mediated mutagenesis of *PLAGL2* in SW480 cells (**R**). Statistical significance (*p<0.05 or **p<0.01) was evaluated through an ordinary one-way ANOVA and Dunnett's multiple comparisons post-hoc test.

DISCUSSION

We find that PLAGL2 is a transcriptional regulator of cellular transformation in colorectal cancer, being able to drive hallmark features, including unchecked proliferation, migration, invasion, and anchorage independent growth. The normal physiological role of PLAGL2 is likely integral to a developmental pathway considering its high expression in the fetal intestinal anlagen and early postnatal intestine, but low expression in adult tissue [39]. *Plagl2*^{-/-} mice demonstrate defects in intestinal epithelial differentiation and function, suggesting that PLAGL2 plays a critical role during fetal intestinal development [39]. Similar to many other Let-7 targets, such as *HMGA2*, *PLAGL2* appears to exhibit typical features of an onco-fetal gene, considering its frequent re-activation in CRC and other malignancies [20, 28, 40-42]. However, there has been little insight into the role of direct transcriptional targets of PLAGL2, either during fetal development or carcinogenesis. Our current studies here were all conducted *in vitro*, which have many limitations, and validating *in vivo* models should be pursued in the future to delineate the role of PLAGL2 in intestinal mucosal transformation.

In possible oncogenic roles, PLAGL2 has been shown to directly activate transcription of the thrombopoietin receptor (*MPL*) [43], which is a key receptor necessary for megakaryocyte and platelet formation [44]. *MPL* is also a proto-oncogene that can drive hematopoietic cell proliferation when it (or the truncated *v-mpl* oncogene) is over-expressed [45, 46]. Relevant to PLAGL2, *MPL* is implicated in driving transformation downstream of PLAGL2 in acute myeloid leukemia (AML) [43], a malignancy in which increased expression of *MPL* marks a particularly

aggressive subset [47]. However, even though *MPL* has been shown to be expressed on a subset of CRC cells that have metastatic tropism for the liver and lung [48, 49], *MPL* expression is not induced by *PLAGL2* in intestinal organoids [20] and *MPL* expression does not correlate with *PLAGL2* expression in CRC [29]. Thus, *MPL* may not be a relevant oncogenic *PLAGL2* target gene in CRC. Other potential *PLAGL2* targets, such as *NIP3* and *P73* [50, 51], appear to have tumor-suppressive properties, while another documented target, surfactant protein C (*SPC*) [52], has unknown relevance to tumorigenesis and/or cellular transformation.

We have previously identified *ASCL2* as a direct target gene of *PLAGL2*. *ASCL2* is a bHLH transcription factor that directly supports *LGR5* expression [22], drives IESC fate [21, 22, 53], and promotes an aggressive phenotype in CRC [53-55]. Regarding this effect in CRC, *ASCL2* represses expression of *CDX2*, a transcription factor with a well-described role in positively driving intestinal epithelial differentiation [54]. *ASCL2* also represses expression of miR-200 miRNAs, which may underlie effects on a mesenchymal phenotype and/or EMT in cancer, which is repressed by the miR-200 family of miRNAs [55]. Studies have also suggested that *ASCL2* may play a role in augmenting the tumor-initiating capacity of CRC cells [56, 57], although this has not yet been carefully examined. Ultimately, the role of *ASCL2* may prove to be pleiotropic, as these studies suggest, with variable effects on differentiation, EMT, and tumor initiating potential.

Surprisingly, in our studies, *ASCL2* over-expression confers a survival disadvantage to *PLAGL2* mutants in the Caco2 cell line, even though we see that cell cycle progression is promoted by *ASCL2* rescue in the context of *PLAGL2* knock-down. Thus, *ASCL2* alone may have different effects than when co-expressed with *PLAGL2* at high levels; such effects of *ASCL2* may repress cellular transformation when *PLAGL2* levels are low. Previous studies seeking to identify *ASCL2* co-immunoprecipitating proteins included the identification of *PLAGL2*, as determined by mass spectrometry [38], although such direct interaction was not verified by other methods. If direct interaction can occur between these factors, then the effects

we see on the STAR-tdT reporter in CRC cell lines could possibly reflect direct roles for PLAGL2 on ASCL2-responsive regulatory elements. While follow-up studies are needed, PLAGL2 and ASCL2 may biochemically cooperate to drive specific oncogenic targets – targets that may differ from those that are transcriptionally activated individually by each individual factor.

For effects on tumorigenesis, a gain-of-function role for ASCL2 (e.g. in the context of ASCL2 up-regulation) is not clear. Modest entopic over-expression of *Ascl2*, at levels 2-3-fold higher than non-transgenic mice, via a BAC transgene, does not accelerate CRC tumorigenesis in the context of the *Apc^{Min}* allele [58], a tumor model in which mice develop adenomatous polyps in the small intestine and colon. However, DNA replication (as measured by bromodeoxyuridine incorporation) is significantly elevated in the intestinal epithelium of these *Ascl2* transgenic mice, suggesting that elevated levels of ASCL2 can drive cell cycle progression [58]. Consistent with these *in vivo* findings, we observe accelerated cell cycle progression following ASCL2 over-expression in the context of PLAGL2 knock-down. In contrast to SW480 cells, which express very low levels of ASCL2 mRNA and protein, Caco2 cells express very high levels of ASCL2 [54]. Thus, ASCL2 may play a differential role downstream of PLAGL2, depending on the individual tumor or cancer cell line. In light of *in vivo* studies described above, ASCL2 may only have cancer-promoting effects when PLAGL2 is also coordinately up-regulated and/or activated. The co-expression of PLAGL2 with ASCL2 is striking in CRC [20], so the context for cooperation certainly exists in tumors.

The PLAGL2 paralog, PLAG1, is reported to transcriptionally activate the IGF2 promoter [34, 36], with over-expression experiments in NIH-3T3 and HEK293 cells suggesting that PLAGL2 may also positively regulate IGF2 expression. IGF2 (a known driver of tumor progression) is over-expressed in ~15% of CRCs and also activates the PI3K-AKT pathway [59-65]. IGF2 up-regulation also occurs in the context of wild-type *PTEN*, *PIK3CA*, *BRAF*, and *KRAS* [29], suggesting that IGF2 over-expression can functionally substitute for common PI3K-

AKT-activating mutations. Here we provide data in primary intestinal organoids and human CRC cell lines that *PLAGL2* is necessary and sufficient to drive *IGF2* expression. Following knock-out or knock-down of *PLAGL2* in CRC cell lines, we observe that *IGF2* expression is depleted up to 95%, and in a CRC cell line such as Caco2, which is known to express very high levels of IGF2 [66-68]), severe reduction of IGF2 has consequential effects on cellular growth. Evidence for this exists through studies of Caco2 cells, which are sensitive to both a neutralizing anti-IGF2 antibody [66] and an IGF1R/INSR inhibitor [68], which blocks IGF2 or the receptors through which IGF2 signals, respectively. However, we cannot rescue cellular proliferation and/or survival following *PLAGL2* mutagenesis in Caco2 cells via over-expression of IGF2. Thus, the growth defects caused by *PLAGL2* loss are due to other effectors, besides IGF2. In *PLAGL2* mutant DLD1 cells *ASCL2* and IGF2 each alone have modest effects on clone proliferation, but cooperative/synergistic effects when co-expressed. Therefore, in some contexts these *PLAGL2* targets cooperate, whereas in other contexts, such as Caco2 cells, we do not see evidence of cooperation. Thus, the oncogenic dependency of *PLAGL2* on IGF2 and *ASCL2* is context-dependent, varying between tumors and/or tumor types.

Finally, our data suggest a minor role for Wnt signaling downstream of *PLAGL2* in CRC. While previous studies indicate that *WNT6* is a *PLAGL2* target gene [27, 28], and our previous studies show that *PLAGL2* activates the expression of Wnt genes (i.e. *Wnt9b*, *Wnt4*, *Wnt10a*, and *Wnt5a*) in primary intestinal epithelial cells [20], our studies here in CRC cell lines indicate that canonical Wnt signaling (via TCF4/ β -Catenin) are only modestly affected by *PLAGL2*. Additionally, in available data from TCGA we find that *PLAGL2* levels do not correlate with a Wnt signature, as measured by the induction of Wnt target genes. If the effects of *PLAGL2* on Wnt signaling are routed via Wnt ligands (such as *WNT6*), then a minor effect on Wnt activation is not unexpected, since the vast majority of colorectal cancers possess mutations in either *APC*, *AXIN2*, or *CTNNB1* [29] — mutations that lead to ligand-independent Wnt pathway activation. However, an earlier role may exist for Wnt-dependent effects of *PLAGL2* if *PLAGL2*

is activated prior to cell autonomous activation of intrinsic Wnt signaling through such mutations. This is a limitation of our study – the inability to model early pre-cancerous lesions prior such canonical Wnt pathway mutations. Other PLAGL2 target genes, besides Wnt ligands themselves, could be intracellular modifiers of the canonical Wnt signaling pathway. However, given the modest effects of PLAGL2 on canonical Wnt signaling in CRC cells, the net effect of any such hypothetical targets is likely to be relatively small. This underscores the need to identify additional PLAGL2 target genes, especially those involved in fetal growth pathways and carcinogenesis; identifying such targets will help illuminate the onco-fetal pathways downstream of PLAGL2.

MATERIALS AND METHODS

Statistical Analysis

All statistical analyses were performed using GraphPad Prism (Version 8 for Windows, GraphPad Software, San Diego, California USA, www.graphpad.com). Threshold for significance (alpha level) was 0.05 for all tests.

Cell lines

Cell lines used in this study include Caco-2 [Caco2] (ATCC® HTB-37™), HT29 [HT-29] (ATCC® HTB-38™), SW480 [SW-480] (ATCC® CCL-228™), DLD1 [DLD-1] (ATCC® CCL-221™), and IEC6 [IEC-6] (ATCC® CRL-1592™). Cells were cultured in media prescribed by ATCC with the inclusion of a prophylactic dose of Plasmocin (Invivogen) to prevent mycoplasma contamination.

Ethics statements

Colorectal tumor specimens were provided by the Siteman Cancer Center Tissue Procurement Core, Human Studies Institutional Review Board number 201106191. These tissues were fully anonymized prior to accessing them, thus an individual IRB was not required.

Mice are housed in the fully AAALAC/OLAW certified animal facility at the Washington University in St. Louis School of Medicine. Mice are housed in a 12 hour light/dark cycle with free access to food and water; the number of mice per cage was as mandated by the Institutional Animal Care and Use Committee (IACUC) of Washington University in St. Louis School of Medicine to ensure humane caging. All animal experimentation was approved by the IACUC/ Animal Studies Committee of Washington University School of Medicine as stated in approved protocol # IACUC 20170164.

Euthanasia was performed by CO₂ asphyxiation with a flow control gauge followed by cervical dislocation as recommended and approved for mice by the American Veterinary Medical Association Panel on Euthanasia and by the IACUC and Division of Comparative Medicine at Washington University in St. Louis School of Medicine.

RT-PCR

CRC tumor samples, along with paired non-cancerous controls, were obtained from Siteman Cancer Center Tissue Procurement Core and were previously described [10]. RNA was extracted with TRIzol (ThermoFisher Scientific) and further purified using the RNeasy RNA Clean-up Kit (Qiagen) for these tumor samples. For cell lines or enteroids, RNA was prepared using TRIzol. RT reactions were performed with 3-4 µg total RNA using oligo-dT and SuperScript III RT (ThermoFisher Scientific). QPCR was performed as previously described [20], and expression levels normalized to *PPIA* and *B2M* for human specimens or human cell

lines. For RT-PCR using RNA from mouse organoids or cell lines expression levels were normalized to *Hprt* and *Tbp*.

TCGA analysis

TCGA data was examined using the cBioPortal for Cancer Genomics [30, 31], hosted by the Center for Molecular Oncology at MSKCC. Oncoprint analysis (Fig 1D) was performed for CRC AdCA tumors from the PanCan study [73]. Overall survival rates among CRC patients from the TCGA were determined from analysis of microarray data from two cohorts parsed for expression of *PLAGL2*. For one CRC dataset [29] *PLAGL2*-high tumors were those with greater than 3 SD above the mean for *PLAGL2* expression, while another CRC dataset (TCGA-provisional) *PLAGL2*-high tumors were defined as those with greater than 2 SD above the mean for *PLAGL2* expression and *PLAGL2*-low tumors were defined as those with more than 0.25 SD below the mean for *PLAGL2* expression.

PLAGL2 mutagenesis with CRISPR/eSpCas9 and

SRIRACCHA

For expression of eSpCas9 [74], the ORF from eSpCas9 was amplified from eSpCas9(1.1), which was a gift from Feng Zhang (Addgene plasmid # 71814) and cloned into BII-ChBtW, which is identical to BII-ChPtW (which confers Puromycin resistance through PAC), but confers Blasticidin resistance. Using 8 μ L Lipofectamine 2000 (ThermoFisher Scientific) this vector, BII-ChBtW-eSpCas9, was introduced into Caco2 and HT29 cells by transfecting 1.6 μ g of transposon along with 400 ng of pCMV-hyPBBase [75], a generous gift from Dr. Allan Bradley (Wellcome Sanger Institute). Selection with 10 μ g/ml Blasticidin was initiated 48 hours after transfection and continued for 7 days, whereupon cells were expanded for transfection with BII-

gR-PnGW. The BII-gR-PnGW vector contains a U6-driven gRNA cassette cloned from pX335, which was a gift from Feng Zhang (Addgene plasmid # 42335, [76]). This U6-driven gRNA module was cloned 5' of the CMV/hEf1a promoter at a unique *SfiI* site, and was modified to contain two *BsmBI* sites for cloning gRNA oligos, in place of the existing *BbsI* sites. The BII-gR-PnGW also constitutively expresses GFP-NLS for visualization of transduced cells. Transfections of the BII-gR-PnGW vector were performed in quadruplicate in 24-well plates 24 hours after plating 5×10^4 cells per well. Cells were transfected as above using 400 ng BII-gR-PnGW and 100 ng pCMV-hyPBase, selected with 5 μ g/mL Puromycin for 4 days (HT29) or 10 μ g/mL Puromycin for 10 days (Caco2). Fluorescence was measured starting 48 hours after transfection. A non-specific gRNA (GGAGACGCTGACCCGTCTCT) was used as a control for comparison with a PLAGL2-targeting gRNA (GTTACCGCAAGGACCATCTG) [20]. SRIRACCHA-mediated mutagenesis was performed using the BII-gR-PtW-eSpCas9 vector, which contains a gRNA-expression cassette (as in BII-gR-PnGW) and confers resistance to Puromycin. SW480 (8×10^5 cells) or Caco2 (3×10^5 cell) were plated in triplicate or quadruplicate in 6-well plates 24 hours prior to transfection. For one-step transfection with SRIRACCHA components, 600 ng of the BII-gR-PtW-eSpCas9 vector with gRNAs specific for either PLAGL2 (GTTACCGCAAGGACCATCTG) or LacZ (GAAGGCGGCGGGCCATTACC) were transfected along with 600 ng of the BII-C3H target vector [32] containing target sequences either for PLAGL2 or LacZ cloned at the 3' end of the PAC ORF, 500 ng of pBS-PtH, and 300 ng of pCMV-hyPBase. SW480 cells were transfected using JetPrime (Polyplus Inc.) (2 μ L/ μ g DNA) per manufacturer instructions while Caco2 cells were transfected using Lipofectamine 2000 (ThermoFisher Inc.) (4 μ L/ μ g DNA) per manufacturer instructions. Cells were selected with Puromycin for 5 days, then switched to Hygromycin selection for 10 days. RNA was then isolated using TRIzol or, alternatively, both RNA and DNA were isolated using the Allprep DNA/RNA Mini Kit (Qiagen Inc.). Mutation analysis was performed either on cDNA (SW480) or gRNA (Caco2). Mutation of *PLAGL2* was determined by amplicon sequencing on

the Illumina platform by the Center for Genomic Sciences (Washington University) and analysis was performed using CRISPResso [77]. For transfection with SRIRACCHA components in rescue experiments, Caco2 cells were transfected in a one- or two-step manner. For the two-step method, 3×10^5 cells in a 6-well plate that had been seeded the previous day were transfected with 800 ng BII-C3H-PLAGL2-T1 vector containing the PLAGL2 targeting gRNA sequence, 800 ng of either BII-ChBtW (empty vector), BII-ChBtW-ASCL2 (overexpressing ASCL2), or BII-ChBtW-IGF2 (overexpressing *IGF2*), and 400 of pCMV-hyPBase. Transfection medium was removed in 24 hours and replaced with growth medium. Growth medium was changed in a further 24 hours for 10 μ g/mL Puromycin and 10 μ g/mL Blasticidin containing growth medium, and cells were selected for resistance for 8 days with regular media changes. Once cells reached confluency again, they were trypsinized and removed from the plate, and 3×10^5 cells were again seeded, this time into three identical wells of a 6-well plate. The following day, cells were transfected with 1,600 ng of the BII-gR-PtW-eSpCas9-PLAGL2-T1R vector, the Cas9 activity surrogate vector, 750 ng of the pBS-PtH vector, which contains the hygromycin resistance cassette, and 250 ng of pCMV-hyPBase. Transfection medium was removed and changed as before, and 48 hours post transfection medium containing 400 μ g/mL Hygromycin was added. Cells were selected for Hygromycin resistance for 13 days.

For the one-step method, 3×10^5 cells seeded the previous day into a 6-well plate were transfected with 400 ng BII-C3H-PLAGL2-T1 vector containing the PLAGL2 targeting gRNA sequence, 400 ng of either BII-ChBtW (empty vector), BII-ChBtW-ASCL2 (overexpressing ASCL2), or BII-ChBtW-IGF2 (overexpressing *IGF2*), 500 ng of the BII-gR-PtW-eSpCas9-PLAGL2-T1R vector, 300 ng of the pBS-PtH vector, and 400 ng of the pCMV-hyPBase vector. Transfection medium was removed and changed again in 24 hours, and 48 hours post transfection cells were selected with 10 μ g/mL Puromycin and 10 μ g/mL Blasticidin for 5 days, before changing to medium containing 400 μ g/mL Hygromycin for 11 days.

For both methods, after Hygromycin selection was finished (cells reached confluency), gDNA was extracted and mutation of *PLAGL2* was again determined by amplicon sequencing on the Illumina platform by the Center for Genomic Sciences (Washington University) and subsequent analysis by CRISPResso.

Cell proliferation assays

Cellular proliferation was quantified by automated microscopy of GFP-positive cells on a Biotek Cytation3 using a 4x objective, where cell numbers were gauged by enumerating individual cells or by quantifying total integrated fluorescence per well. DLD1 *PLAGL2* mutants [20] express H2BGFP while other cell lines express nuclear GFP following stable transfection with BII-ShPnGW or BII-gR-PnGW. Cellular fluorescence was imaged every 1-2 days and media changed every 2-3 days.

Cell cycle analysis with FUCCI reporter

A *Piggybac* version of the FUCCI reporter (BII-ChPtW-iresFUCCI) was constructed by PCR amplification of the Clover-Geminin-ires-mKO2-Cdt fragment from pLL3.7 (Addgene Plasmid #83841, [33]) and insertion into unique *BsmBI* sites within the *Piggybac* vector BII-ChPtW. The BII-ChPtW vector was constructed by insertion of the Woodchuck Hepatitis Virus (WHP) Posttranscriptional Regulatory Element (WPRE) downstream of the *BsmBI* site in the previously described BII-ChPt vector [20]. Transfections of the BII-ChPtW-iresFUCCI vector were performed in quadruplicate in 24-well plates 24 hours after plating 5×10^4 cells per well. Cells were transfected as above using 400 ng of PB transposon and 100 ng pCMV-hyPBase, selected with 5 $\mu\text{g/mL}$ Puromycin for 4 days (HT29) or 10 $\mu\text{g/mL}$ Puromycin for 10 days (Caco2).

PLAGL2 shRNA-mediated knockdown

For protein knockdown, an shRNA expression *Piggybac* vector, BII-ShPnGW was constructed by insertion of a GFP-NLS cDNA into the *BsmBI* cloning sites of BII-ChPtW. A U6-driven shRNA module was then inserted at a unique *SfiI* site upstream of the CMV/hEf1a promoter, with *BsmBI* cloning sites for insertion of unique shRNA double-stranded oligos. The BII-ShPiRW vector was constructed for FUCCI experiments. This vector is identical to BII-ShPnGW, but expresses the iRFP702 near-IR protein [78], which was first codon optimized, synthesized and cloned from a gBlock fragment (IDT Inc.). Alternatively, for rescue experiments (Fig 6), the shRNA module from BII-ShPnGW was cloned as an *NsiI*-*AgeI* fragment into those unique restriction sites in BII-ChPtW-iresFUCCI to generate BII-Sh-FUCCI. The Broad Gene Perturbation Portal was queried for identification of candidate shRNAs against *PLAGL2*, and oligos prepared identical to the strategy employed for shRNA expression from the pLKO.1 vector [79], except overhangs were modified for directional cloning into our BII-ShPnGW vector, with 5' overhangs ACCG and AAAA at the termini of each dsDNA oligo. The following four *PLAGL2*-specific target sequences were cloned in this manner: shRNA #1: TTCAGGCTCTAGGATCGATTC, shRNA #2: CCGTAGGACTTCAGGTATTAT, shRNA #3: TTGGATGACCTCTAGAGAAAT, shRNA #4: GCAGGAGAGAAGGCCTTTATT. A luciferase-specific shRNA was used as a control, with target sequence TCACAGAATCGTCGTATGCAG. The BII-ShPnGW vector with each specific shRNA was transfected into DLD1 cells in triplicate in 6-well plates, with 1.6 µg of transposon transfected along with 400 ng of pCMV-hyPBase. Selection was initiated 48 hours after transfection using 10 µg/mL Puromycin for Caco2 cells, or 5 µg/mL for other cell lines, and continued for 4-7 days. Cells were then cultured for 1-2 days in medium without Puromycin prior to harvesting RNA or protein for RT-PCR or immunoblot.

Migration and invasion assays

For migration assays 1×10^5 cells were plated in 0.5 mL DMEM in Falcon Fluoroblok trans-well inserts containing 8 μ m pores, which were placed into Falcon 24-well plates, with each well containing 0.75 mL DMEM and 10% FBS. Plates were cultured 24 to 48 hours and then imaged for GFP fluorescence using the Biotek Cytation3. For invasion assays Falcon Fluoroblok trans-well inserts were coated with cold 25% Matrigel (75% DMEM), which was then solidified for one hour at 37°C. Cells were then added to transwell inserts and cultured and imaged as above for migration assays. DLD1 mutant clones (#1 and #2) and parental cells express H2BGFP for visualization [20], while the shRNA knock-down vector (BII-ShPnGW) provided nuclear-localized GFP for enumeration of migratory cells by microscopy using the Biotek Cytation3.

Soft agar colony formation assays

IEC6 cells were cultured in Advanced-DMEM/F12 (ThermoFisher Inc.) containing 5% FBS, Glutamax (ThermoFisher Inc.), HEPES, N2 Supplement (ThermoFisher Inc.), Plasmocin (Invivogen Inc.), and Penicillin/Streptomycin. Over-expression vectors were prepared by cloning the PLAGL2 coding sequence into BII-ChBtW and IEC6 cells transfected in 6 well plates with 1600 ng of this plasmid and 400 ng of pCMV-hyPBase using Lipofectamine 2000 (ThermoFisher Inc.). Cells were select 48 hours after transfection with medium containing 4 μ g/ml Blasticidin and selected for 5 days. To assay anoikis resistance and anchorage-independent proliferation IEC6 cells were grown in 0.35% low-melt agarose (Lonza SeaPlaque). A base layer of agarose was prepared by melting pre-sterilized 1.2% agarose in dH₂O at 75°C, and cooling for 60 minutes at 42°C. This was then mixed with pre-heated 0.22 μ m-filtered 2x DMEM containing 20% FBS, Sodium Bicarbonate, Sodium Pyruvate, Glutamax (ThermoFisher Inc.), HEPES, 2x N2 Supplement (ThermoFisher Inc.), Plasmocin (Invivogen Inc.), and Penicillin/Streptomycin. This mixture (1 mL) was applied to the bottom of an ultra-low

attachment 6-well plate (Greiner Bio-One Inc.) and allowed to cool for 5 minutes at room temperature. Cells were detached with 0.05% Trypsin-EDTA and counted and placed on ice. Pre-sterilized 0.7% agarose was prepared as above, equilibrated for 60 minutes at 42°C, and mixed with pre-warmed growth medium, and then incubated 30 minutes at 37°C. Cells (8×10^4) were added to 3.2 mL of this 0.35% agarose, mixed well, and then 1 mL over-layered onto each well containing a base layer of 0.6% agarose in 6-well plates. Plates were then incubated 20 minutes at room temperature and then placed into a 37°C incubator with 6% CO₂. The next day 1 mL of complete culture medium was added. Colonies were counted 3 weeks following plating.

Organoid culture and transfection

Mouse small intestine organoids (enteroids) were generated from jejunum crypts from three (3) C57BL/6 mice (8-12 weeks) obtained from Jackson Laboratory, and cultured and transfected as previously described [20]. *Plagl2* mutant/KO and PLAGL2 over-expressing (O/E) mouse enteroids were previously described [20]. IGF2 O/E enteroids were generated by cloning the human IGF2 ORF into the BII-ChBtW vector via *BsmBI* sites, and transfection in mouse enteroids using 800 ng of this BII-ChBtW-IGF2 vector along with 200 ng of pCMV-hyPBase. Enteroid transfections were performed as previously described [20]. Multiple (n=20-50) Blasticidin-resistance clones were obtained and pooled for stable propagation of a polyclonal line. IGF2 expression was assayed by RT-PCR and morphology documented using the Cytation3 microscopy platform and a 4x objective.

ASCL2 and Wnt reporter assays

The ASCL2 reporter was previously described [38]. Briefly, this reporter was adapted for *Piggybac* transposon-mediated gene delivery by cloning ASCL2 regulatory elements downstream of 2 polyadenylation signals (one synthetic and one from the SV40 TK gene) and

upstream of a tandem tomato (tdT) fluorescent protein ORF and NLS signal, followed by the bovine growth hormone (bGH) polyadenylation signal, all flanked by HSIV core insulators from the chicken *HBBA* gene. For transfection, SW480 (2×10^5 cells), HT29 (2×10^5 cells), or Caco2 (1×10^5 cells) were plated in triplicate or quadruplicate in 24-well plates 24 hours prior to transfection. Cells were transfected with 200 ng of BII-STAR-tdT, 200 ng of BII-ShPnGW, and 100 ng of pCMV-hyPBase. The BII-ShPnGW vector contained shRNA sequences directed against a non-specific target or the *PLAGL2* mRNA, as described above. For a positive control of reporter activity BII-STAR-tdT was co-transfected with 200 ng of BII-ChBtW-ASCL2 for ASCL2 O/E. Red fluorescence was quantified 48 hours after transfection using the Cytation3 platform. Cells were then selected with Puromycin for 5 days and then both GFP and RFP fluorescence were quantified using the Cytation3. The BII-TOP-tdT reporter for the canonical Wnt pathway was described previously [20], but was modified for nuclear expression with a C-terminal NLS. This vector was transfected and visualized in SW480, HT29, and Caco2 cells as described above for BII-STAR-tdT. For a positive control of this fluorescent Wnt reporter, BII-ChBtW-dnTCF4 was co-transfected with BII-TOP-tdT. This dominant negative TCF4 variant was described previously [80] and was modified here for expression via transposon. Red fluorescence was quantified 48 hours after transfection using the Cytation3 (Agilent-Biotek Inc.) platform and subsequently after antibiotic selection, as described above for the BII-STAR-tdT reporter.

FUCCI rescue experiments

For rescuing cell cycle effects caused by *PLAGL2* knockdown the FUCCI vector was modified for simultaneous shRNA expression by cloning the *NsiI* – *AgeI* fragment from BII-ShPnGW, which includes shRNA components, into BII-ChPtW-iresFUCCI to create the BII-shFUCCI vector. Caco2 were plated in quadruplicate for transfection with BII-shFUCCI along

with BII-ChBtW vectors for O/E of PLAGL2, ASCL2, IGF2, or CTNNB1^{S33Y}. The constitutively active beta-catenin mutant (CTNNB1^{S33Y}) was described previously [81]. Beginning 48 hours after transfection cells were selected with Puromycin and Blasticidin for 5 days and then RFP and GFP fluorescence were quantified using the Cytation3.

Immunoblots and protein quantification

For analysis of active and total β -Catenin levels upon *PLAGL2* mRNA KD, Caco2 and SW480 cells in a 6 well dish were transfected with the shRNA construct and selected as previously described, in triplicate. After the initial selection and subsequent expansion of cells to near confluency, cells were harvested and lysate was extracted using Cell Lysis Buffer (Cell Signaling Technology) according to manufacturer's specifications. Briefly, a 1X concentration of this buffer was made with the addition of 2X protease inhibitor cocktail (Millipore Sigma), 1 mM sodium fluoride, 1 mM sodium pyrophosphate, and 5 mM activated sodium orthovanadate. Cells were rinsed in 1x PBS in the plate, add 500 μ L of the lysis buffer was added. The plate was incubated on ice for 5 minutes. The cells and buffer were then removed to a 1.7 mL microcentrifuge tube and sonicated for 10 seconds. Tubes were centrifuged at 14,000 x g for 10 minutes, and supernatant was removed to a separate tube. Protein concentration was determined using a microplate and BCA assay kit (Thermofisher) as per manufacturer's specifications. Equal amounts of protein (nominally 50 μ g) from each sample were separated on 4-20% gradient Bis-Tris SDS-PAGE gels (GenScript), and protein was then electroblotted onto low autofluorescence PVDF membrane (Bio-Rad). The membrane was blocked in 1X PBS + 5% BSA (Millipore Sigma), and probed overnight with primary rabbit antibodies raised against total or active β -Catenin (Cell Signaling Technology, #8480 and #8814 respectively), and primary mouse antibodies raised against α -tubulin (Santa Cruz Biotechnology #sc-5286) as a loading control. The next day, the primary antibodies were washed off and the blot was

incubated with goat anti-mouse DyLight 680 conjugated (ThermoFisher #35518) and goat anti-rabbit DyLight 800 (Thermofisher #SA5-10036) conjugated secondary antibodies for an hour. The secondary antibodies were washed off and signal was captured using the LiCor Odyssey CLx Near-Infrared Imaging System, using the 800 channel to capture β -Catenin signal and the 700 channel to capture α -tubulin signal. Quantitation of signal was performed using ImageStudio Lite (LiCor), using the software's "average" method of background subtraction. β -Catenin signal was normalized using α -tubulin signal, and average normalized β -Catenin signal, standard deviation, and statistical significance were calculated and plotted using GraphPad Prism 8.

Acknowledgements

We thank the Alvin J. Siteman Cancer Center at Washington University School of Medicine and Barnes-Jewish Hospital in St. Louis, MO. and the Institute of Clinical and Translational Sciences (ICTS) at Washington University in St. Louis, for the use of the Tissue Procurement Core, which provided colon adenocarcinoma and non-malignant tissue samples.

References

1. MacDonald BT, Tamai K, He X. Wnt/beta-catenin signaling: components, mechanisms, and diseases. *Dev Cell*. 2009;17(1):9-26. Epub 2009/07/22. doi: S1534-5807(09)00257-3 [pii] 10.1016/j.devcel.2009.06.016. PubMed PMID: 19619488.
2. Kinzler KW, Nilbert MC, Su LK, Vogelstein B, Bryan TM, Levy DB, et al. Identification of FAP locus genes from chromosome 5q21. *Science*. 1991;253(5020):661-5. Epub 1991/08/09. doi: 10.1126/science.1651562. PubMed PMID: 1651562.

- 721 3. Seshagiri S, Stawiski EW, Durinck S, Modrusan Z, Storm EE, Conboy CB, et al.
722 Recurrent R-spondin fusions in colon cancer. *Nature*. 2012;488(7413):660-4. doi:
723 10.1038/nature11282. PubMed PMID: 22895193; PubMed Central PMCID: PMC3690621.
- 724 4. Ben-Porath I, Thomson MW, Carey VJ, Ge R, Bell GW, Regev A, et al. An embryonic
725 stem cell-like gene expression signature in poorly differentiated aggressive human tumors. *Nat*
726 *Genet*. 2008;40(5):499-507. doi: 10.1038/ng.127. PubMed PMID: 18443585; PubMed Central
727 PMCID: PMC2912221.
- 728 5. Merlos-Suarez A, Barriga FM, Jung P, Iglesias M, Cespedes MV, Rossell D, et al. The
729 intestinal stem cell signature identifies colorectal cancer stem cells and predicts disease
730 relapse. *Cell Stem Cell*. 2011;8(5):511-24. doi: 10.1016/j.stem.2011.02.020. PubMed PMID:
731 21419747.
- 732 6. Johnson CD, Esquela-Kerscher A, Stefani G, Byrom M, Kelnar K, Ovcharenko D, et al.
733 The let-7 microRNA represses cell proliferation pathways in human cells. *Cancer Res*.
734 2007;67(16):7713-22. Epub 2007/08/19. doi: 67/16/7713 [pii]
735 10.1158/0008-5472.CAN-07-1083. PubMed PMID: 17699775.
- 736 7. Gurtan AM, Ravi A, Rahl PB, Bosson AD, JnBaptiste CK, Bhutkar A, et al. Let-7
737 represses Nr6a1 and a mid-gestation developmental program in adult fibroblasts. *Genes Dev*.
738 2013;27(8):941-54. doi: 10.1101/gad.215376.113. PubMed PMID: 23630078; PubMed Central
739 PMCID: PMC3650230.
- 740 8. Boyerinas B, Park SM, Shomron N, Hedegaard MM, Vinther J, Andersen JS, et al.
741 Identification of let-7-regulated oncofetal genes. *Cancer Res*. 2008;68(8):2587-91. Epub
742 2008/04/17. doi: 68/8/2587 [pii]
743 10.1158/0008-5472.CAN-08-0264. PubMed PMID: 18413726.
- 744 9. Boyerinas B, Park SM, Hau A, Murmann AE, Peter ME. The role of let-7 in cell
745 differentiation and cancer. *Endocr Relat Cancer*. 2010;17(1):F19-36. doi: 10.1677/ERC-09-
746 0184. PubMed PMID: 19779035.

- 747 10. Madison BB, Jeganathan AN, Mizuno R, Winslow MM, Castells A, Cuatrecasas M, et al.
748 Let-7 Represses Carcinogenesis and a Stem Cell Phenotype in the Intestine via Regulation of
749 Hmga2. PLoS Genet. 2015;11(8):e1005408. doi: 10.1371/journal.pgen.1005408. PubMed
750 PMID: 26244988; PubMed Central PMCID: PMC4526516.
- 751 11. King CE, Wang L, Winograd R, Madison BB, Mongroo PS, Johnstone CN, et al. LIN28B
752 fosters colon cancer migration, invasion and transformation through let-7-dependent and -
753 independent mechanisms. Oncogene. 2011;30(40):4185-93. Epub 2011/06/01. doi:
754 10.1038/onc.2011.131. PubMed PMID: 21625210; PubMed Central PMCID: PMC3165068.
- 755 12. Madison BB, Liu Q, Zhong X, Hahn CM, Lin N, Emmett MJ, et al. LIN28B promotes
756 growth and tumorigenesis of the intestinal epithelium via Let-7. Genes Dev. 2013;27(20):2233-
757 45. doi: 10.1101/gad.224659.113. PubMed PMID: 24142874; PubMed Central PMCID:
758 PMC3814644.
- 759 13. Kumar MS, Erkeland SJ, Pester RE, Chen CY, Ebert MS, Sharp PA, et al. Suppression
760 of non-small cell lung tumor development by the let-7 microRNA family. Proc Natl Acad Sci U S
761 A. 2008;105(10):3903-8. Epub 2008/03/01. doi: 0712321105 [pii]
762 10.1073/pnas.0712321105. PubMed PMID: 18308936.
- 763 14. Yu F, Yao H, Zhu P, Zhang X, Pan Q, Gong C, et al. let-7 regulates self renewal and
764 tumorigenicity of breast cancer cells. Cell. 2007;131(6):1109-23. doi: 10.1016/j.cell.2007.10.054.
765 PubMed PMID: 18083101.
- 766 15. Ricarte-Filho JC, Fuziwara CS, Yamashita AS, Rezende E, da-Silva MJ, Kimura ET.
767 Effects of let-7 microRNA on Cell Growth and Differentiation of Papillary Thyroid Cancer. Transl
768 Oncol. 2009;2(4):236-41. Epub 2009/12/04. PubMed PMID: 19956384.
- 769 16. Nadiminty N, Tummala R, Lou W, Zhu Y, Shi XB, Zou JX, et al. MicroRNA let-7c is
770 downregulated in prostate cancer and suppresses prostate cancer growth. PLoS One.
771 2012;7(3):e32832. Epub 2012/04/06. doi: 10.1371/journal.pone.0032832. PubMed PMID:
772 22479342; PubMed Central PMCID: PMC3316551.

17. Qian P, Zuo Z, Wu Z, Meng X, Li G, Wu Z, et al. Pivotal role of reduced let-7g expression in breast cancer invasion and metastasis. *Cancer Res.* 2011;71(20):6463-74. doi: 10.1158/0008-5472.CAN-11-1322. PubMed PMID: 21868760.
18. Ye S, Song W, Xu X, Zhao X, Yang L. IGF2BP2 promotes colorectal cancer cell proliferation and survival through interfering with RAF-1 degradation by miR-195. *FEBS Lett.* 2016;590(11):1641-50. doi: 10.1002/1873-3468.12205. PubMed PMID: 27153315.
19. Wang X, Liu X, Li AY, Chen L, Lai L, Lin HH, et al. Overexpression of HMGA2 promotes metastasis and impacts survival of colorectal cancers. *Clin Cancer Res.* 2011;17(8):2570-80. doi: 10.1158/1078-0432.CCR-10-2542. PubMed PMID: 21252160; PubMed Central PMCID: PMC3079060.
20. Strubberg AM, Veronese Paniagua DA, Zhao T, Dublin L, Pritchard T, Bayguinov PO, Fitzpatrick JAJ, Madison BB. The Zinc Finger Transcription Factor PLAGL2 Enhances Stem Cell Fate and Activates Expression of ASCL2 in Intestinal Epithelial Cells. *Stem Cell Reports.* 2018 Aug 14;11(2):410-424. doi: 10.1016/j.stemcr.2018.06.009. Epub 2018 Jul 12. PMID: 30017821; PMCID: PMC6092695.
21. van der Flier LG, van Gijn ME, Hatzis P, Kujala P, Haegebarth A, Stange DE, et al. Transcription factor achaete scute-like 2 controls intestinal stem cell fate. *Cell.* 2009;136(5):903-12. Epub 2009/03/10. doi: S0092-8674(09)00079-8 [pii] 10.1016/j.cell.2009.01.031. PubMed PMID: 19269367.
22. Schuijers J, Junker JP, Mokry M, Hatzis P, Koo BK, Sasselli V, et al. Ascl2 acts as an R-spondin/Wnt-responsive switch to control stemness in intestinal crypts. *Cell Stem Cell.* 2015;16(2):158-70. doi: 10.1016/j.stem.2014.12.006. PubMed PMID: 25620640.
23. Wang YP, Guo PT, Zhu Z, Zhang H, Xu Y, Chen YZ, et al. Pleomorphic adenoma gene like-2 induces epithelial-mesenchymal transition via Wnt/beta-catenin signaling pathway in

- 797 human colorectal adenocarcinoma. *Oncol Rep.* 2017. doi: 10.3892/or.2017.5485. PubMed
798 PMID: 28259923.
- 799 24. Zhou J, Liu H, Zhang L, Liu X, Zhang C, Wang Y, et al. DJ-1 promotes colorectal cancer
800 progression through activating PLAGL2/Wnt/BMP4 axis. *Cell Death Dis.* 2018;9(9):865. Epub
801 2018/08/31. doi: 10.1038/s41419-018-0883-4. PubMed PMID: 30158634; PubMed Central
802 PMCID: PMCPMC6115399.
- 803 25. Liu X, Chen X, Zeng K, Xu M, He B, Pan Y, et al. DNA-methylation-mediated silencing of
804 miR-486-5p promotes colorectal cancer proliferation and migration through activation of
805 PLAGL2/IGF2/beta-catenin signal pathways. *Cell Death Dis.* 2018;9(10):1037. Epub
806 2018/10/12. doi: 10.1038/s41419-018-1105-9. PubMed PMID: 30305607; PubMed Central
807 PMCID: PMCPMC6180105.
- 808 26. Li D, Lin C, Li N, Du Y, Yang C, Bai Y, et al. PLAGL2 and POFUT1 are regulated by an
809 evolutionarily conserved bidirectional promoter and are collaboratively involved in colorectal
810 cancer by maintaining stemness. *EBioMedicine.* 2019;45:124-38. Epub 2019/07/08. doi:
811 10.1016/j.ebiom.2019.06.051. PubMed PMID: 31279780; PubMed Central PMCID:
812 PMCPMC6642334.
- 813 27. Li N, Li D, Du Y, Su C, Yang C, Lin C, et al. Overexpressed PLAGL2 transcriptionally
814 activates Wnt6 and promotes cancer development in colorectal cancer. *Oncol Rep.*
815 2019;41(2):875-84. Epub 2018/12/12. doi: 10.3892/or.2018.6914. PubMed PMID: 30535429;
816 PubMed Central PMCID: PMCPMC6313070.
- 817 28. Zheng H, Ying H, Wiedemeyer R, Yan H, Quayle SN, Ivanova EV, et al. PLAGL2
818 regulates Wnt signaling to impede differentiation in neural stem cells and gliomas. *Cancer Cell.*
819 2010;17(5):497-509. doi: 10.1016/j.ccr.2010.03.020. PubMed PMID: 20478531; PubMed
820 Central PMCID: PMC2900858.

29. Cancer Genome Atlas N. Comprehensive molecular characterization of human colon and rectal cancer. *Nature*. 2012;487(7407):330-7. doi: 10.1038/nature11252. PubMed PMID: 22810696; PubMed Central PMCID: PMC3401966.
30. Cerami E, Gao J, Dogrusoz U, Gross BE, Sumer SO, Aksoy BA, et al. The cBio cancer genomics portal: an open platform for exploring multidimensional cancer genomics data. *Cancer discovery*. 2012;2(5):401-4. doi: 10.1158/2159-8290.CD-12-0095. PubMed PMID: 22588877; PubMed Central PMCID: PMC3956037.
31. Gao J, Aksoy BA, Dogrusoz U, Dresdner G, Gross B, Sumer SO, et al. Integrative analysis of complex cancer genomics and clinical profiles using the cBioPortal. *Sci Signal*. 2013;6(269):pl1. doi: 10.1126/scisignal.2004088. PubMed PMID: 23550210; PubMed Central PMCID: PMC4160307.
32. Wen Y, Liao G, Pritchard T, Zhao TT, Connelly JP, Pruett-Miller SM, et al. A Stable but Reversible Integrated Surrogate Reporter for Assaying CRISPR/Cas9-Stimulated Homology-directed Repair. *J Biol Chem*. 2017. doi: 10.1074/jbc.M117.777722. PubMed PMID: 28228480.
33. Bajar BT, Lam AJ, Badiie RK, Oh YH, Chu J, Zhou XX, et al. Fluorescent indicators for simultaneous reporting of all four cell cycle phases. *Nat Methods*. 2016;13(12):993-6. Epub 2016/11/01. doi: 10.1038/nmeth.4045. PubMed PMID: 27798610; PubMed Central PMCID: PMC5548384.
34. Akhtar M, Holmgren C, Gondor A, Vesterlund M, Kanduri C, Larsson C, et al. Cell type and context-specific function of PLAG1 for IGF2 P3 promoter activity. *Int J Oncol*. 2012;41(6):1959-66. doi: 10.3892/ijo.2012.1641. PubMed PMID: 23023303; PubMed Central PMCID: PMC3583874.
35. Hensen K, Van Valckenborgh IC, Kas K, Van de Ven WJ, Voz ML. The tumorigenic diversity of the three PLAG family members is associated with different DNA binding capacities. *Cancer Res*. 2002;62(5):1510-7. PubMed PMID: 11888928.

36. Voz ML, Agten NS, Van de Ven WJ, Kas K. PLAG1, the main translocation target in pleomorphic adenoma of the salivary glands, is a positive regulator of IGF-II. *Cancer Res.* 2000;60(1):106-13. PubMed PMID: 10646861.
37. Medico E, Russo M, Picco G, Cancelliere C, Valtorta E, Corti G, et al. The molecular landscape of colorectal cancer cell lines unveils clinically actionable kinase targets. *Nat Commun.* 2015;6:7002. doi: 10.1038/ncomms8002. PubMed PMID: 25926053.
38. Oost KC, van Voorthuisen L, Fumagalli A, Lindeboom RGH, Sprangers J, Omerzu M, et al. Specific Labeling of Stem Cell Activity in Human Colorectal Organoids Using an ASCL2-Responsive Minigene. *Cell Rep.* 2018;22(6):1600-14. doi: 10.1016/j.celrep.2018.01.033. PubMed PMID: 29425513; PubMed Central PMCID: PMC5847189.
39. Van Dyck F, Braem CV, Chen Z, Declercq J, Deckers R, Kim BM, et al. Loss of the Plagl2 transcription factor affects lacteal uptake of chylomicrons. *Cell metabolism.* 2007;6(5):406-13. doi: 10.1016/j.cmet.2007.09.010. PubMed PMID: 17983586.
40. Landrette SF, Kuo YH, Hensen K, Barjesteh van Waalwijk van Doorn-Khosrovani S, Perrat PN, Van de Ven WJ, et al. Plag1 and Plagl2 are oncogenes that induce acute myeloid leukemia in cooperation with Cbfb-MYH11. *Blood.* 2005;105(7):2900-7. doi: 10.1182/blood-2004-09-3630. PubMed PMID: 15585652.
41. Liu B, Lu C, Song YX, Gao P, Sun JX, Chen XW, et al. The role of pleomorphic adenoma gene-like 2 in gastrointestinal cancer development, progression, and prognosis. *International journal of clinical and experimental pathology.* 2014;7(6):3089-100. PubMed PMID: 25031728; PubMed Central PMCID: PMC4097215.
42. Guo J, Wang M, Wang Z, Liu X. Overexpression of Pleomorphic Adenoma Gene-Like 2 Is a Novel Poor Prognostic Marker of Prostate Cancer. *PLoS One.* 2016;11(8):e0158667. doi: 10.1371/journal.pone.0158667. PubMed PMID: 27537362; PubMed Central PMCID: PMC4990332.

43. Landrette SF, Madera D, He F, Castilla LH. The transcription factor PlagL2 activates Mpl transcription and signaling in hematopoietic progenitor and leukemia cells. *Leukemia*. 2011;25(4):655-62. doi: 10.1038/leu.2010.301. PubMed PMID: 21263445; PubMed Central PMCID: PMC3076538.
44. de Sauvage FJ, Hass PE, Spencer SD, Malloy BE, Gurney AL, Spencer SA, et al. Stimulation of megakaryocytopoiesis and thrombopoiesis by the c-Mpl ligand. *Nature*. 1994;369(6481):533-8. doi: 10.1038/369533a0. PubMed PMID: 8202154.
45. Souyri M, Vigon I, Penciolelli JF, Heard JM, Tambourin P, Wendling F. A putative truncated cytokine receptor gene transduced by the myeloproliferative leukemia virus immortalizes hematopoietic progenitors. *Cell*. 1990;63(6):1137-47. doi: 10.1016/0092-8674(90)90410-g. PubMed PMID: 2175677.
46. Skoda RC, Seldin DC, Chiang MK, Peichel CL, Vogt TF, Leder P. Murine c-mpl: a member of the hematopoietic growth factor receptor superfamily that transduces a proliferative signal. *EMBO J*. 1993;12(7):2645-53. PubMed PMID: 8334987; PubMed Central PMCID: PMC413511.
47. Vigon I, Dreyfus F, Melle J, Viguie F, Ribrag V, Cocault L, et al. Expression of the c-mpl proto-oncogene in human hematologic malignancies. *Blood*. 1993;82(3):877-83. PubMed PMID: 8393355.
48. Gao W, Chen L, Ma Z, Du Z, Zhao Z, Hu Z, et al. Isolation and phenotypic characterization of colorectal cancer stem cells with organ-specific metastatic potential. *Gastroenterology*. 2013;145(3):636-46 e5. doi: 10.1053/j.gastro.2013.05.049. PubMed PMID: 23747337.
49. Wu Z, Wei D, Gao W, Xu Y, Hu Z, Ma Z, et al. TPO-Induced Metabolic Reprogramming Drives Liver Metastasis of Colorectal Cancer CD110+ Tumor-Initiating Cells. *Cell Stem Cell*. 2015;17(1):47-59. doi: 10.1016/j.stem.2015.05.016. PubMed PMID: 26140605.

- 896 50. Mizutani A, Furukawa T, Adachi Y, Ikehara S, Taketani S. A zinc-finger protein,
897 PLAGL2, induces the expression of a proapoptotic protein Nip3, leading to cellular apoptosis. J
898 Biol Chem. 2002;277(18):15851-8. doi: 10.1074/jbc.M111431200. PubMed PMID: 11832486.
- 899 51. Hanks TS, Gauss KA. Pleomorphic adenoma gene-like 2 regulates expression of the
900 p53 family member, p73, and induces cell cycle block and apoptosis in human promonocytic
901 U937 cells. Apoptosis. 2012;17(3):236-47. doi: 10.1007/s10495-011-0672-3. PubMed PMID:
902 22076304.
- 903 52. Guo Y, Yang MC, Weissler JC, Yang YS. PLAGL2 translocation and SP-C promoter
904 activity--a cellular response of lung cells to hypoxia. Biochem Biophys Res Commun.
905 2007;360(3):659-65. doi: 10.1016/j.bbrc.2007.06.106. PubMed PMID: 17618602; PubMed
906 Central PMCID: PMCPMC2084061.
- 907 53. Giakountis A, Moulos P, Zarkou V, Oikonomou C, Harokopos V, Hatzigeorgiou AG, et al.
908 A Positive Regulatory Loop between a Wnt-Regulated Non-coding RNA and ASCL2 Controls
909 Intestinal Stem Cell Fate. Cell Rep. 2016;15(12):2588-96. doi: 10.1016/j.celrep.2016.05.038.
910 PubMed PMID: 27292638.
- 911 54. Shang Y, Pan Q, Chen L, Ye J, Zhong X, Li X, et al. Achaete scute-like 2 suppresses
912 CDX2 expression and inhibits intestinal neoplastic epithelial cell differentiation. Oncotarget.
913 2015;6(31):30993-1006. doi: 10.18632/oncotarget.5206. PubMed PMID: 26307678; PubMed
914 Central PMCID: PMC4741583.
- 915 55. Tian Y, Pan Q, Shang Y, Zhu R, Ye J, Liu Y, et al. MicroRNA-200 (miR-200) cluster
916 regulation by achaete scute-like 2 (Ascl2): impact on the epithelial-mesenchymal transition in
917 colon cancer cells. J Biol Chem. 2014;289(52):36101-15. doi: 10.1074/jbc.M114.598383.
918 PubMed PMID: 25371200; PubMed Central PMCID: PMC4276874.
- 919 56. Ye J, Liu S, Shang Y, Chen H, Wang R. R-spondin1/Wnt-enhanced Ascl2 autoregulation
920 controls the self-renewal of colorectal cancer progenitor cells. Cell Cycle. 2018;17(8):1014-25.

- doi: 10.1080/15384101.2018.1469874. PubMed PMID: 29886802; PubMed Central PMCID: PMCPMC6103697.
57. Wei X, Ye J, Shang Y, Chen H, Liu S, Liu L, et al. Ascl2 activation by YAP1/KLF5 ensures the self-renewability of colon cancer progenitor cells. *Oncotarget*. 2017;8(65):109301-18. doi: 10.18632/oncotarget.22673. PubMed PMID: 29312609; PubMed Central PMCID: PMCPMC5752522.
58. Reed KR, Tunster SJ, Young M, Carrico A, John RM, Clarke AR. Entopic overexpression of Ascl2 does not accelerate tumourigenesis in ApcMin mice. *Gut*. 2012;61(10):1435-8. doi: 10.1136/gutjnl-2011-300842. PubMed PMID: 22138533.
59. Cui H, Cruz-Correa M, Giardiello FM, Hutcheon DF, Kafonek DR, Brandenburg S, et al. Loss of IGF2 imprinting: a potential marker of colorectal cancer risk. *Science*. 2003;299(5613):1753-5. doi: 10.1126/science.1080902. PubMed PMID: 12637750.
60. Kaneda A, Wang CJ, Cheong R, Timp W, Onyango P, Wen B, et al. Enhanced sensitivity to IGF-II signaling links loss of imprinting of IGF2 to increased cell proliferation and tumor risk. *Proc Natl Acad Sci U S A*. 2007;104(52):20926-31. doi: 10.1073/pnas.0710359105. PubMed PMID: 18087038; PubMed Central PMCID: PMC2409243.
61. Sakatani T, Kaneda A, Iacobuzio-Donahue CA, Carter MG, de Boer Witzel S, Okano H, et al. Loss of imprinting of Igf2 alters intestinal maturation and tumorigenesis in mice. *Science*. 2005;307(5717):1976-8. Epub 2005/02/26. doi: 1108080 [pii] 10.1126/science.1108080. PubMed PMID: 15731405.
62. Zanella ER, Galimi F, Sassi F, G. M, Cottino F, Leto SM, et al. IGF2 is an actionable target that identifies a distinct subpopulation of colorectal cancer patients with marginal response to anti-EGFR therapies. *Sci Transl Med*. 2015;7(272):272ra12. Epub 1/28/2015. doi: 10.1126.

- 945 63. Kinouchi Y, Hiwatashi N, Higashioka S, Nagashima F, Chida M, Toyota T. Relaxation of
946 imprinting of the insulin-like growth factor II gene in colorectal cancer. *Cancer Lett.*
947 1996;107(1):105-8. PubMed PMID: 8913273.
- 948 64. Nishihara S, Hayashida T, Mitsuya K, Schulz TC, Ikeguchi M, Kaibara N, et al. Multipoint
949 imprinting analysis in sporadic colorectal cancers with and without microsatellite instability. *Int J*
950 *Oncol.* 2000;17(2):317-22. PubMed PMID: 10891541.
- 951 65. Nakagawa H, Chadwick RB, Peltomaki P, Plass C, Nakamura Y, de La Chapelle A. Loss
952 of imprinting of the insulin-like growth factor II gene occurs by biallelic methylation in a core
953 region of H19-associated CTCF-binding sites in colorectal cancer. *Proc Natl Acad Sci U S A.*
954 2001;98(2):591-6. doi: 10.1073/pnas.011528698. PubMed PMID: 11120891; PubMed Central
955 PMCID: PMC14632.
- 956 66. Zhong H, Fazenbaker C, Chen C, Breen S, Huang J, Yao X, et al. Overproduction of
957 IGF-2 drives a subset of colorectal cancer cells, which specifically respond to an anti-IGF
958 therapeutic antibody and combination therapies. *Oncogene.* 2016. doi: 10.1038/onc.2016.248.
959 PubMed PMID: 27399333.
- 960 67. Berg KCG, Eide PW, Eilertsen IA, Johannessen B, Bruun J, Danielsen SA, et al. Multi-
961 omics of 34 colorectal cancer cell lines - a resource for biomedical studies. *Mol Cancer.*
962 2017;16(1):116. doi: 10.1186/s12943-017-0691-y. PubMed PMID: 28683746; PubMed Central
963 PMCID: PMC5498998.
- 964 68. Sanderson MP, Hofmann MH, Garin-Chesa P, Schweifer N, Wernitznig A, Fischer S, et
965 al. The IGF1R/INSR Inhibitor BI 885578 Selectively Inhibits Growth of IGF2-Overexpressing
966 Colorectal Cancer Tumors and Potentiates the Efficacy of Anti-VEGF Therapy. *Mol Cancer*
967 *Ther.* 2017;16(10):2223-33. doi: 10.1158/1535-7163.MCT-17-0336. PubMed PMID: 28729397.
- 968 69. Cancer Genome Atlas Research N, Weinstein JN, Collisson EA, Mills GB, Shaw KR,
969 Ozenberger BA, et al. The Cancer Genome Atlas Pan-Cancer analysis project. *Nat Genet.*

- 2013;45(10):1113-20. doi: 10.1038/ng.2764. PubMed PMID: 24071849; PubMed Central
PMCID: PMCPMC3919969.
70. Mokry M, Hatzis P, Schuijers J, Lansu N, Ruzius FP, Clevers H, et al. Integrated
genome-wide analysis of transcription factor occupancy, RNA polymerase II binding and steady-
state RNA levels identify differentially regulated functional gene classes. *Nucleic Acids Res.*
2012;40(1):148-58. doi: 10.1093/nar/gkr720. PubMed PMID: 21914722; PubMed Central
PMCID: PMC3245935.
71. Muta Y, Fujita Y, Sumiyama K, Sakurai A, Taketo MM, Chiba T, et al. Composite
regulation of ERK activity dynamics underlying tumour-specific traits in the intestine. *Nat*
Commun. 2018;9(1):2174. doi: 10.1038/s41467-018-04527-8. PubMed PMID: 29872037;
PubMed Central PMCID: PMCPMC5988836.
72. Veeman MT, Slusarski DC, Kaykas A, Louie SH, Moon RT. Zebrafish *prickle*, a
modulator of noncanonical Wnt/Fz signaling, regulates gastrulation movements. *Curr Biol.*
2003;13(8):680-5. PubMed PMID: 12699626.
73. Hoadley KA, Yau C, Hinoue T, Wolf DM, Lazar AJ, Drill E, et al. Cell-of-Origin Patterns
Dominate the Molecular Classification of 10,000 Tumors from 33 Types of Cancer. *Cell.*
2018;173(2):291-304 e6. doi: 10.1016/j.cell.2018.03.022. PubMed PMID: 29625048; PubMed
Central PMCID: PMCPMC5957518.
74. Slaymaker IM, Gao L, Zetsche B, Scott DA, Yan WX, Zhang F. Rationally engineered
Cas9 nucleases with improved specificity. *Science.* 2016;351(6268):84-8. doi:
10.1126/science.aad5227. PubMed PMID: 26628643; PubMed Central PMCID: PMC4714946.
75. Yusa K, Zhou L, Li MA, Bradley A, Craig NL. A hyperactive piggyBac transposase for
mammalian applications. *Proceedings of the National Academy of Sciences of the United States*
of America. 2011;108(4):1531-6. Epub 2011/01/06. doi: 10.1073/pnas.1008322108. PubMed
PMID: 21205896; PubMed Central PMCID: PMC3029773.

76. Cong L, Ran FA, Cox D, Lin S, Barretto R, Habib N, et al. Multiplex genome engineering using CRISPR/Cas systems. *Science*. 2013;339(6121):819-23. doi: 10.1126/science.1231143. PubMed PMID: 23287718; PubMed Central PMCID: PMC3795411.
77. Pinello L, Canver MC, Hoban MD, Orkin SH, Kohn DB, Bauer DE, et al. Analyzing CRISPR genome-editing experiments with CRISPResso. *Nat Biotechnol*. 2016;34(7):695-7. Epub 2016/07/13. doi: 10.1038/nbt.3583. PubMed PMID: 27404874; PubMed Central PMCID: PMC5242601.
78. Shcherbakova DM, Verkhusha VV. Near-infrared fluorescent proteins for multicolor in vivo imaging. *Nat Methods*. 2013;10(8):751-4. doi: 10.1038/nmeth.2521. PubMed PMID: 23770755; PubMed Central PMCID: PMC3737237.
79. Moffat J, Grueneberg DA, Yang X, Kim SY, Kloepper AM, Hinkle G, et al. A lentiviral RNAi library for human and mouse genes applied to an arrayed viral high-content screen. *Cell*. 2006;124(6):1283-98. doi: 10.1016/j.cell.2006.01.040. PubMed PMID: 16564017.
80. Korinek V, Barker N, Morin PJ, van Wichen D, de Weger R, Kinzler KW, et al. Constitutive transcriptional activation by a beta-catenin-Tcf complex in APC-/- colon carcinoma. *Science*. 1997;275(5307):1784-7. Epub 1997/03/21. PubMed PMID: 9065401.
81. Kolligs FT, Hu G, Dang CV, Fearon ER. Neoplastic transformation of RK3E by mutant beta-catenin requires deregulation of Tcf/Lef transcription but not activation of c-myc expression. *Mol Cell Biol*. 1999;19(8):5696-706. PubMed PMID: 10409758; PubMed Central PMCID: PMC84421.

Supporting information

Fig S1. Indel and substitution mutations in SW480 cells around three target SRIRACCHA based CRISPR/Cas9 cleavage sites in *PLAGL2*. A) Mutation distribution around cleavage sites in *PLAGL2* gene with NS gRNA, showing no events. **B)** Mutation distribution around the

PLAGL2 Drives Colorectal Epithelial Transformation Via Wnt-Independent Pathways 42

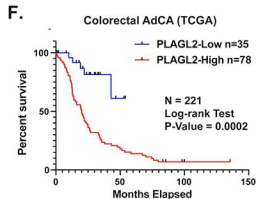
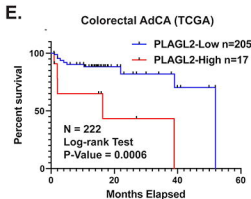
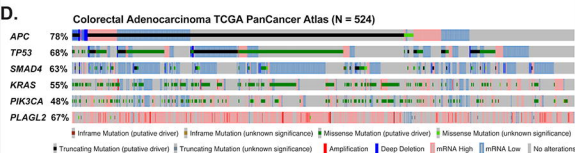
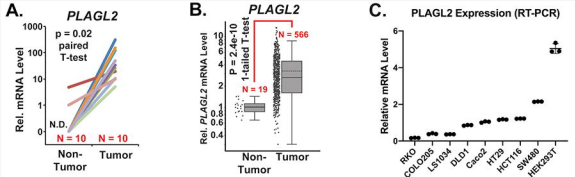
1020 three target cleavage sites in *PLAGL2* **C**) Example allele profile of SRIRACCHA reads from

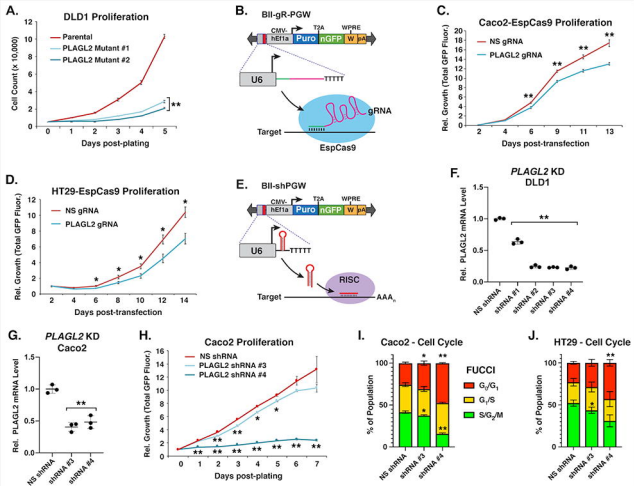
1021 these *PLAGL2* mutations. Note, the top hit represents unmodified *PLAGL2*.

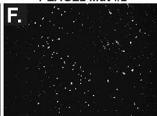
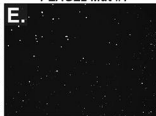
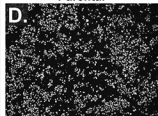
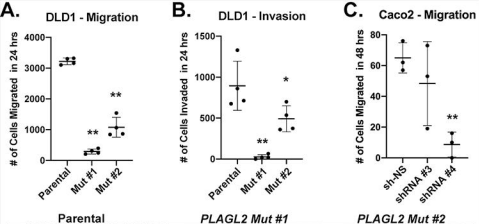
1022 Original Western blot images and raw data used for calculations (means, statistics, etc.)

1023 can be found at <https://wustl.box.com/s/288v1qk8ksiqxl4wyufy44mtq4tj2c3p>.

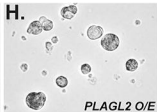
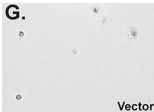
1024

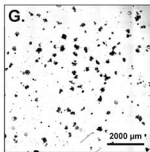
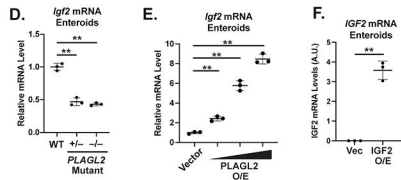
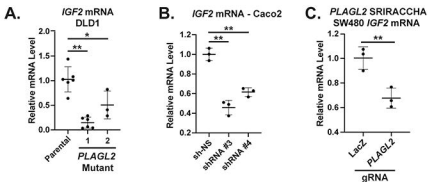




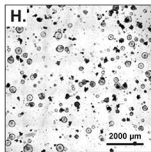


IEC6
Soft
Agar
Colony
Form.

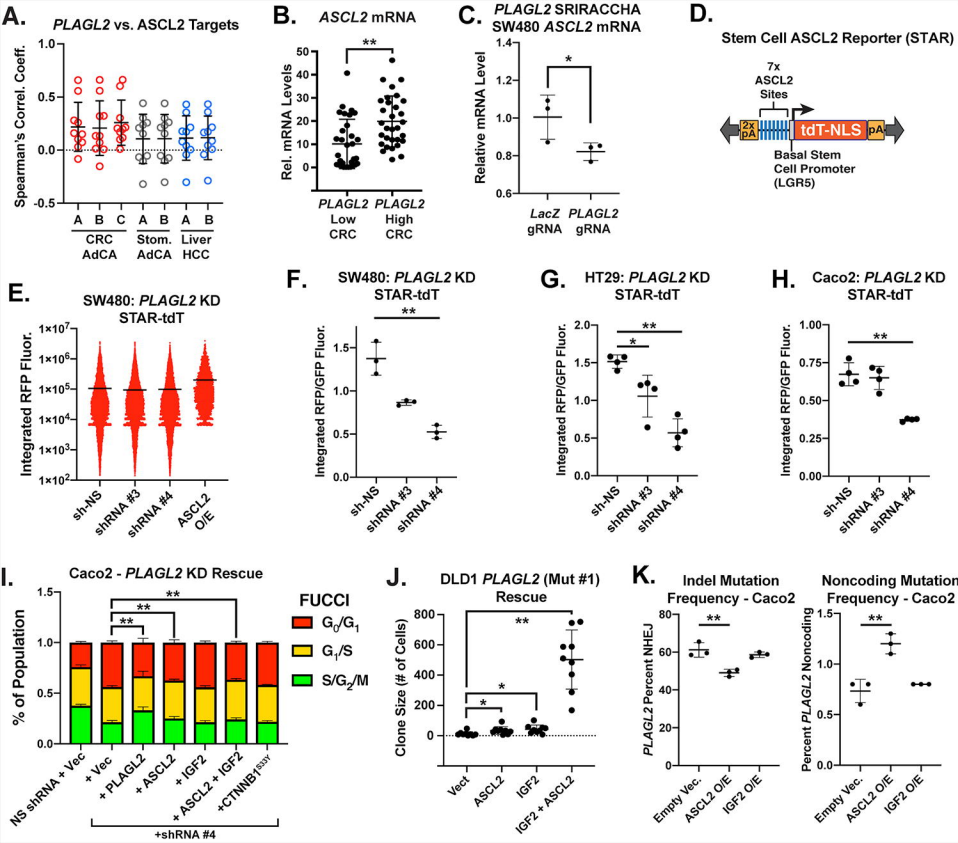


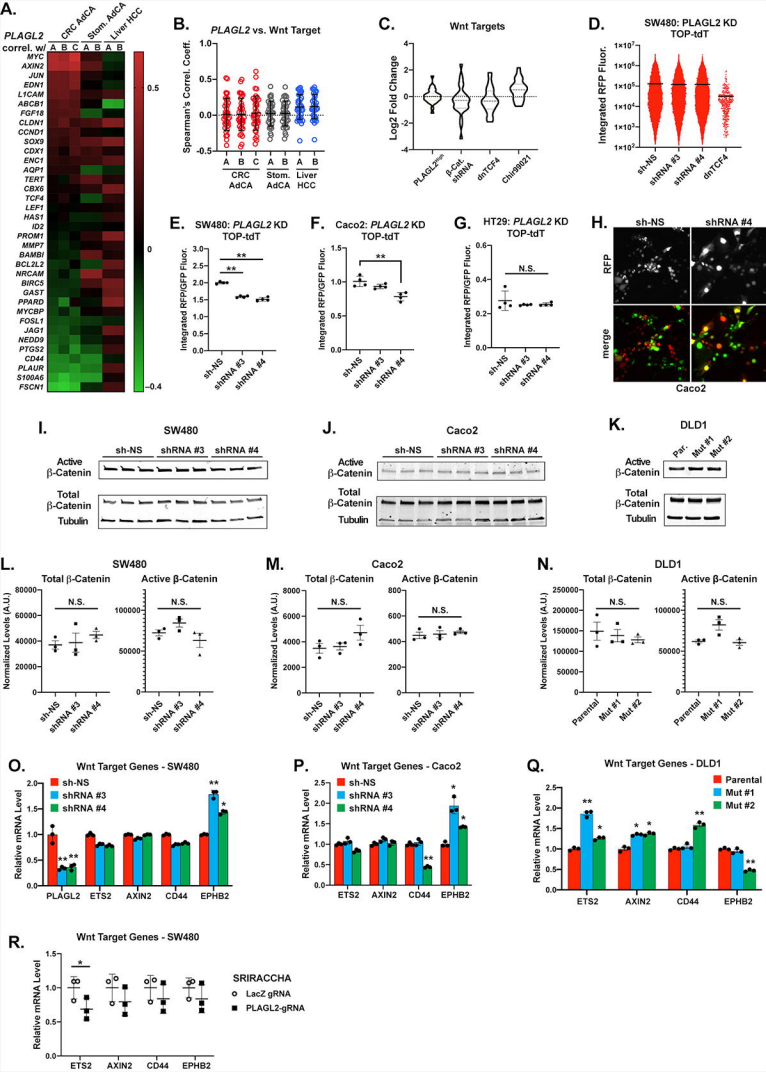


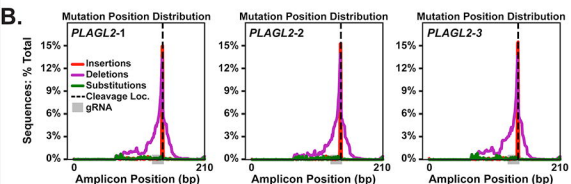
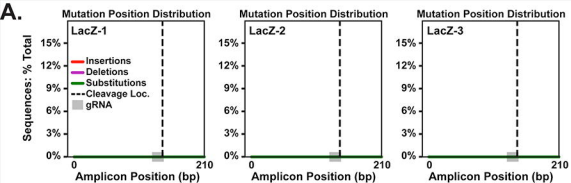
Empty Vector



IGF2 O/E







C. --- = Cleavage Location = Insertions (–) = Deletions **Bold** = Substitutions

T	G	T	T	C	A	C	C	G	C	A	A	G	G	A	C	C	A	T	C	T	G	C	G	G	A	A	C	C	A	T	C	T	G	C	A	G	A	C	Reference
T	G	T	T	C	A	C	C	G	C	A	A	G	G	A	C	C	A	T	C	T	G	C	G	G	A	A	C	C	A	T	C	T	G	C	A	G	A	51.08% (93546 reads)	
T	G	T	T	C	A	C	C	G	C	A	A	G	G	A	C	C	A	T	C	T	G	C	G	G	A	A	C	C	A	T	C	T	G	C	A	G	A	12.96% (23738 reads)	
T	G	T	T	C	A	C	C	G	C	A	-	-	-	-	-	-	-	T	C	T	G	C	G	G	A	A	C	C	A	T	C	T	G	C	A	G	A	2.44% (4466 reads)	
T	G	T	T	C	A	C	C	G	C	A	A	G	G	A	C	C	A	T	C	T	G	C	G	G	A	A	C	C	A	T	C	T	G	C	A	G	A	2.33% (4260 reads)	
T	G	T	T	C	A	C	C	G	C	A	A	G	G	A	C	C	A	T	C	T	G	C	G	G	A	A	C	C	A	T	C	T	G	C	A	G	A	2.10% (3841 reads)	
T	G	T	T	C	A	C	C	G	C	A	A	G	G	A	C	C	A	T	C	T	G	C	G	G	A	A	C	C	A	T	C	T	G	C	A	G	A	2.04% (3727 reads)	
T	G	T	T	C	A	C	C	G	C	A	A	G	G	A	C	C	A	T	C	T	G	C	G	G	A	A	C	C	A	T	C	T	G	C	A	G	A	1.99% (3641 reads)	
T	G	T	T	C	A	C	C	G	C	A	A	G	G	A	C	C	A	T	C	T	G	C	G	G	A	A	C	C	A	T	C	T	G	C	A	G	A	1.56% (2856 reads)	
T	G	T	T	C	A	C	C	G	C	A	A	G	G	A	C	C	A	T	C	T	G	C	G	G	A	A	C	C	A	T	C	T	G	C	A	G	A	1.19% (2171 reads)	
T	G	T	T	C	A	C	C	G	C	A	A	G	G	A	C	C	A	T	C	T	G	C	-	-	-	-	-	-	-	-	-	-	-	-	-	-	0.98% (1788 reads)		
T	G	T	T	C	A	C	C	G	C	A	A	G	G	A	C	C	A	T	C	T	G	C	G	G	A	A	C	C	A	T	C	T	G	C	A	G	A	0.90% (1640 reads)	
T	G	T	T	C	A	C	C	G	C	A	A	G	G	A	C	C	A	T	C	T	G	C	G	G	A	A	C	C	A	T	C	T	G	C	A	G	A	0.89% (1622 reads)	
T	G	T	T	C	A	C	C	G	C	A	A	G	G	A	C	C	A	T	C	T	G	C	-	-	-	-	-	-	-	-	-	-	-	-	-	-	0.87% (1597 reads)		
T	G	T	T	C	A	C	C	-	-	-	-	-	-	-	-	-	-	A	T	C	T	G	C	G	G	A	A	C	C	A	T	C	T	G	C	A	G	A	0.71% (1297 reads)
T	G	T	T	C	A	C	C	G	C	A	A	G	G	A	C	C	A	T	C	T	G	C	G	G	A	A	C	C	A	T	C	T	G	C	A	G	A	0.66% (1217 reads)	
T	G	T	T	C	A	C	C	G	C	A	A	-	-	-	-	-	-	C	A	T	C	T	G	C	G	A	A	C	C	A	T	C	T	G	C	A	G	A	0.66% (1200 reads)
T	G	T	T	C	A	C	C	G	C	A	A	-	-	-	-	-	-	-	-	-	-	-	-	-	-	-	-	-	-	-	-	-	-	-	-	-	0.63% (1145 reads)		
T	G	T	T	C	A	C	C	G	C	A	A	-	-	-	-	-	-	-	-	-	-	-	-	-	-	-	-	-	-	-	-	-	-	-	-	-	0.62% (1128 reads)		
T	G	T	T	C	A	-	-	-	-	-	-	-	-	-	-	-	-	A	T	C	T	G	C	G	G	A	A	C	C	A	T	C	T	G	C	A	G	A	0.54% (984 reads)
T	G	T	T	C	A	C	-	-	-	-	-	-	-	-	-	-	-	-	-	-	-	-	-	-	-	-	-	-	-	-	-	-	-	-	-	-	0.45% (833 reads)		
T	G	T	T	C	A	C	C	G	C	A	A	G	G	A	C	C	A	T	C	T	G	C	G	G	A	A	C	C	A	T	C	T	G	C	A	G	A	0.45% (823 reads)	
T	G	T	T	C	A	C	C	G	C	A	A	G	G	A	C	C	A	T	C	T	G	C	G	G	A	A	C	C	A	T	C	T	G	C	A	G	A	0.42% (778 reads)	
T	G	T	T	C	A	C	-	-	-	-	-	-	-	-	-	-	-	A	T	C	T	G	C	G	G	A	A	C	C	A	T	C	T	G	C	A	G	A	0.41% (756 reads)
T	G	T	T	C	A	C	C	G	C	A	A	G	G	A	C	C	A	T	C	T	G	C	G	G	A	A	C	C	A	T	C	T	G	C	A	G	A	0.37% (671 reads)	
T	G	T	T	C	A	C	C	G	C	-	-	-	-	-	-	-	-	-	-	-	-	-	-	-	-	-	-	-	-	-	-	-	-	-	-	-	0.36% (667 reads)		
T	T	T	C	A	C	C	T	G	C	A	-	-	-	-	-	-	-	-	-	-	-	-	-	-	-	-	-	-	-	-	-	-	-	-	-	-	0.33% (597 reads)		
T	T	T	C	A	C	C	T	G	C	A	-	-	-	-	-	-	-	-	-	-	-	-	-	-	-	-	-	-	-	-	-	-	-	-	-	-	0.31% (570 reads)		
T	G	T	T	C	A	C	C	G	C	A	A	G	-	-	-	-	-	-	-	-	-	-	-	-	-	-	-	-	-	-	-	-	-	-	-	-	0.29% (539 reads)		
T	G	T	T	C	A	C	C	G	C	A	A	G	G	A	C	C	A	T	C	T	G	C	G	G	A	A	C	C	A	T	C	T	G	C	A	G	A	0.27% (496 reads)	
T	G	T	T	C	A	C	C	G	C	A	A	G	G	A	C	C	A	T	C	T	G	C	-	-	-	-	-	-	-	-	-	-	-	-	-	-	-	0.25% (453 reads)	
T	G	T	T	C	A	C	C	G	C	A	A	-	-	-	-	-	-	-	-	-	-	-	-	-	-	-	-	-	-	-	-	-	-	-	-	-	0.24% (441 reads)		
T	G	T	T	C	A	C	C	G	C	A	A	-	-	-	-	-	-	-	-	-	-	-	-	-	-	-	-	-	-	-	-	-	-	-	-	-	0.23% (425 reads)		
T	G	T	T	C	A	C	C	G	C	A	A	G	G	A	C	C	A	T	C	T	G	C	G	G	A	A	C	C	A	T	C	T	G	C	A	G	A	0.21% (382 reads)	
T	G	T	T	C	A	C	C	G	C	-	-	-	-	-	-	-	-	-	-	-	-	-	-	-	-	-	-	-	-	-	-	-	-	-	-	-	0.21% (377 reads)		
T	G	T	T	C	A	C	-	-	-	-	-	-	-	-	-	-	-	-	-	-	-	-	-	-	-	-	-	-	-	-	-	-	-	-	-	-	0.20% (375 reads)		
G	T	T	C	A	C	C	G	C	A	A	G	G	A	C	C	A	T	C	T	G	C	G	G	A	A	C	C	A	T	C	T	G	C	A	G	A	0.20% (367 reads)		

